

UC Berkeley

Research Reports

Title

Integrated Roadway/Adaptive Cruise Control System: Safety, Performance, Environmental and Near Term Deployment Considerations

Permalink

<https://escholarship.org/uc/item/08b7s26b>

Authors

Ioannou, Petros
Wang, Yun
Chang, Hwan

Publication Date

2007-07-01

CALIFORNIA PATH PROGRAM
INSTITUTE OF TRANSPORTATION STUDIES
UNIVERSITY OF CALIFORNIA, BERKELEY

Integrated Roadway/Adaptive Cruise Control System: Safety, Performance, Environmental and Near Term Deployment Considerations

Petros Ioannou, Yun Wang, Hwan Chang
University of Southern California

**California PATH Research Report
UCB-ITS-PRR-2007-8**

This work was performed as part of the California PATH Program of the University of California, in cooperation with the State of California Business, Transportation, and Housing Agency, Department of Transportation, and the United States Department of Transportation, Federal Highway Administration.

The contents of this report reflect the views of the authors who are responsible for the facts and the accuracy of the data presented herein. The contents do not necessarily reflect the official views or policies of the State of California. This report does not constitute a standard, specification, or regulation.

Final Report for Task Order 5501

July 2007

ISSN 1055-1425

Integrated Roadway/Adaptive Cruise Control System: Safety, Performance, Environmental and Near Term Deployment Considerations¹

Final Report: TO5501

(Continuation for TO4242)

Principal Investigator: Professor Petros Ioannou

Graduate Students: Yun Wang and Hwan Chang

Center for Advanced Transportation Technologies

University of Southern California

EE-Systems, EEB200, MC2562

Los Angeles, CA 90089

March 31, 2007

¹ This work is supported by the California Department of Transportation through PATH of the University of California. The contents of this report reflect the views of the authors who are responsible for the facts and accuracy of the data presented herein. The contents do not necessarily reflect the official views or policies of the State of California or the Federal Highway Administration. This report does not constitute a standard, specification or regulation.

Executive Summary

In this project, we present the design, analysis and performance evaluation of the Integrated Roadway/Adaptive Cruise Control System (IRAC) proposed in Task Order (TO) 4242 and studied further in the continuation of TO4242 under TO5501. The IRAC system is a highway traffic control system which integrates ramp metering strategies and a speed control strategy by taking into account highway to vehicle communication, and adaptive cruise control (ACC) system technologies on board of the vehicles. The IRAC system closes the loop of an almost open loop highway traffic system by controlling both the ramps and the speed distribution along the highway lanes. The speed control and the ramp metering strategies are both extended and generalized versions of ALINEA and are designed based on the fundamental flow-density relationship. Available communication technologies such as Dedicated Short Range Communication (DSRC) systems are shown to be adequate to communicate to vehicles the desired speed limit commands generated by the IRAC system. The IRAC system is evaluated using the I-80 as a site for possible implementation. Real traffic data from the I-80 are used to validate a traffic flow simulation model developed using the software package VISSIM. The validated simulation model is then used to evaluate the IRAC system under different traffic scenarios involving mixed traffic ranging from 0% to 100% ACC vehicles, different traffic flow demands, recurrent and non recurrent disturbances.

The results demonstrate that the IRAC system could lead to a better managed traffic flow system where travel times are improved and the flows are smoother leading to potential improvements in safety and environment. While the magnitude of these improvements depends on the traffic situation and traffic disturbances, our results demonstrate consistent improvements under all scenarios considered. The report concludes by suggesting a stretch of the I-80 as a possible site for implementation due to the existence of traffic sensors as part of the Berkeley Highway Laboratory which minimizes changes to the existing infrastructure.

Keywords: freeway traffic control, ramp metering, speed control, roadside to vehicle communication, microscopic simulation, ACC vehicles.

TABLE OF CONTENTS

LIST OF FIGURES	III
LIST OF TABLES	IV
1 INTRODUCTION	1
2 INTEGRATED ROADWAY/ADAPTIVE CRUISE CONTROL SYSTEM	4
2.1 System Description and Notation	5
2.2 Generalized ALINEA Ramp Metering Strategy	6
2.3 Speed Limit Control Strategy	7
3 ROADWAY TO VEHICLE COMMUNICATION	11
4 MICROSCOPIC SIMULATION MODELING AND VALIDATION	15
4.1 Freeway Model and Field Data	16
4.2 Construction of Freeway Model using VISSIM	17
4.3 Model Validation Results	20
5 DEPLOYMENT SCENARIOS AND EVALUATION	28
5.1 Traffic Scenarios	28
5.2 Evaluation of the IRAC System	29
6 UPGRADING THE IRAC SYSTEM	33
6.1 Effect of ACC Vehicles on Flow-Density Relationship	33
6.2 Controller Simulation Results with ACC Vehicles	37
7 DEPLOYMENT OF THE IRAC SYSTEM	41
8 CONCLUSIONS	42
REFERENCES	43

LIST OF FIGURES

Figure 1. Integrated Roadway/Adaptive Cruise Control (IRAC) System	4
Figure 2. The IRAC as feedback control system	5
Figure 3. A uni-directional freeway divided into N sections	6
Figure 4. Fundamental flow-density diagram.....	10
Figure 5. Strictly increasing mapping from $[Q_{\min}, Q_{\max}]$ to $[V_{\min}, v_c]$	10
Figure 6. ITS Architecture	12
Figure 7. 5.9 GHz DSRC band plan with 10 MHz channels and power limit.....	12
Figure 8. Roadside to vehicle communication system.....	13
Figure 9. DSRC system architecture.....	14
Figure 10. Layout of the extended BHL.....	16
Figure 11. System architecture for the simulations.....	20
Figure 12. Car following model parameter estimation using field data	22
Figure 13. Parameter sensitivity with respect to speed and flow errors	23
Figure 14. (a) Field flow (b) Simulated flow.....	25
Figure 15. (a) Field velocity (b) Simulated velocity.....	26
Figure 16. (a) Field speed-flow relationship (b) Simulated speed-flow relationship.....	27
Figure 17. Speed contours for scenario 1: (a) Without IRAC and (b) With IRAC.....	31
Figure 18. Speed contours for scenario 4: (a) Without IRAC and (b) With IRAC.....	32
Figure 19. Flow-density diagram in mixed ACC scenarios.....	33
Figure 20. Propagation of shock waves (a) 0% ACC vehicles (b) 20% ACC (c) 40% ACC (d) 60% ACC (e) 80% ACC (f) 100% ACC	34
Figure 21. Selected vehicle trajectories (a) 0% ACC vehicles (b) 20% ACC (c) 40% ACC (d) 60% ACC (e) 80% ACC (f) 100% ACC. Red lines represent ACC vehicles and blue lines represent manual vehicles	36
Figure 22. Speed contour of scenario 1 (a) 0% ACC, w/o IRAC (b) 0% ACC, with IRAC (c) 40% ACC, w/o IRAC (d) 40% ACC, with IRAC (e) 100% ACC, w/o IRAC (f) 100% ACC, with IRAC	39
Figure 23. Speed contour of scenario 4 (a) 0% ACC, w/o IRAC (b) 0% ACC, with IRAC (c) 40% ACC, w/o IRAC (d) 40% ACC, with IRAC (e) 100% ACC, w/o IRAC (f) 100% ACC, with IRAC	40
Figure 24. Suggested locations of detector stations and locations of billboards or beacons along the I-80 segment.....	41

LIST OF TABLES

Table 1. Ramp flow rates and placement of controllers	28
Table 2. Controller Parameters	28
Table 3. Simulation inputs for different congestion scenarios	29
Table 4. Shock wave speeds of different traffic composition.....	35
Table 5. All simulation results	38

1 INTRODUCTION

Freeways have been originally built to provide almost unlimited mobility to road users for a number of years to come. No one predicted the dramatic expansion of car ownership which led to the current situation where congestion during rush hours often converts a smooth traffic flow to a virtual parking lot. The negative effects of congestion go beyond the obvious one, the travel time that drivers experience, to include environmental and health effects, travel cost, safety, quality of life, etc. The need for additional capacity in order to maintain the mobility and freedom drivers used to enjoy in the past can no longer be met in most metropolitan areas by following the traditional approach of building additional highways. The lack of space, high cost of land, environmental constraints, and the time it takes to build a new highway as well as the possible disruption to the traffic system in already congested areas makes the building of new highways in many metropolitan areas a very challenging proposition. The only way to add additional capacity is to make the current system more efficient through the use of technologies and intelligence. This approach was advocated by many researchers and Department of Transportation officials and stakeholders over the years. With the Department of Transportation in California as the pioneer the concept of Automated Highway Systems (AHS) emerged and was researched under the PATH program for a number of years [45]. The momentum was strong and soon enough the FHWA and DOT funded the National Consortium for AHS with the task to provide the first demonstration of AHS concepts in 1997. In August of 1997 several demonstrations of AHS concepts took place on I-15 north of San Diego in a highly publicized event [45-54]. Despite the success of the demonstrations the consortium ended shortly after the demonstration and the idea of AHS appeared to be given up by the Federal Government. Concepts such as organization of automated cars in platoons with very small intervehicle spacing were shown to have the potential of increasing current highway capacity by 4 to 5 times providing an amazingly high additional capacity [45-49, 51-54]. Despite this strong potential of increasing capacity, advanced ideas such as automated platoons were considered by some as very far in the future by others as unrealistic systems due to the technical, human factors and liability issues involved which would make every automobile manufacturer shy away from such system. The AHS effort did not achieve its objectives for deployment but stimulated a lot of research and motivated the development of technologies with beneficial effects on transportation. Adaptive cruise control, automatic toll collection, collision warning, new traffic data collection systems, blind spot detection, lane assist systems etc are some of the technologies which appeared in a rather short period of time and contributed to improved safety and positive yet minor improvements on traffic. Despite these improvements the traffic situation on today's highways suffers from many major drawbacks which include the lack of adequate and accurate spatial and temporal measurements of the traffic characteristics and limited subsequent processing and evaluation. The system despite the local ramp metering operates mostly as an open loop dynamical system. As characterized in [1] 'the traffic situation on today's freeways resembles very much the one in urban road networks prior to the introduction of traffic lights: blocked links, chaotic intersections, reduced safety'. In another paper [55] it is pointed out that most of the congestion is due to mismanagement of traffic rather than to

demand exceeding capacity. The current highway system operates as an almost open loop dynamical system which is susceptible to the effect of disturbances in way that leads to frequent congestion phenomena.

During the recent years considerable research efforts have been made to improve the current situation. Among the various traffic flow control strategies, ramp metering, speed control, route guidance and the combination of them have been developed and implemented. According to an overview [1], modern ramp metering strategies could be classified into two categories: (1) Reactive strategies, such as ALINEA [2-4], aiming at maintaining the freeway traffic conditions close to pre-specified set values by use of real-time measurements and (2) Nonlinear optimal ramp metering strategies, such as fuzzy logic, artificial neural networks and other optimal ramp control strategies [5-11]. In addition to ramp metering, variable speed limits can be issued by the infrastructure to vehicles in an effort to control traffic flow characteristics on highways. It has been shown that the use of variable speed limits can improve traffic flow performance [13, 14] by preventing traffic flow breakdown [12] in the presence of traffic disturbances. The coordination of variable speed limits and ramp metering is shown to increase the range ramp metering is effective [16]. Nonlinear optimization and model predictive control (MPC) techniques have been used for generating desired speed limits commands [15, 16].

Most of the control strategies proposed in literature are designed based on certain second-order macroscopic traffic flow models. Since these traffic flow models may change significantly due to changes in a real network, the deployment of the control systems designed based on these models should be carefully evaluated. The design and evaluation of control strategies using simplified macroscopic simulation models which are not accurate enough to regenerate the detailed characteristics of a real freeway network may lead to incorrect control commands with adverse effects on performance. In this project as in our previous work [17, 18], microscopic traffic simulation models validated using real data are used to evaluate the effectiveness and robustness of proposed control strategies.

During the last decade, considerable research efforts have been devoted to automating vehicles in an effort to improve safety and efficiency of vehicle following [19]. While dedicated highways with fully automated vehicles is a far in the future objective [20], the introduction of semi-automated vehicles, such as vehicles with Adaptive Cruise Control (ACC), also referred to as Intelligent Cruise Control (ICC), on current freeways designed to operate with manually driven vehicles has already taken place in Japan and Europe and more recently in the US too [21]. These trends offer an opportunity to have the infrastructure communicate directly with ACC vehicles by providing commands, recommendations and warnings for the purpose of improving traffic flow characteristics and safety. It motivates the design of ACC systems as an integral part of a larger control system that involves the roadway.

The development of an integrated roadway/ACC (IRAC) system that takes into account individual vehicle safety and performance, traffic flow characteristics, and environmental considerations is of importance to the nation's ITS program. Therefore, in our previous research [22], new designs of ACC systems have been developed based on the above

performance considerations. Specifically, based on a simplified longitudinal vehicle model, we design two ACC systems, referred to as ACC01 and ACC02 that can be implemented with any general variable time headway. The ACC01 has similar properties as the ACC systems proposed in the literature whereas ACC02 is different and is equipped with more intelligence when it comes to disturbance rejection and smooth response. ACC02 treats the vehicle following task as a special case of the speed tracking task, and is designed to provide better transient performance by using a nonlinear logic function. We propose and analyze a new variable time headway which is parameterized by a design constant r which is interpreted as the ratio of the time headway used by ACC vehicles versus that of manually driven vehicles. Our study concludes that the ACC02 with the new proposed variable time headway with $r < 1$ provides the best performance with respect to vehicle following, environment and traffic flow characteristics. Safety considerations may require r to be not much less than 1 or an additional technology may be used to improve the reaction time of ACC during braking maneuvers. The ACC02 system is also able to receive speed commands from the roadway and respond in a smooth way without any adverse effect on travel time.

The objective of this research is to develop link layer controllers in order to interface with the ACC vehicles and manual vehicles in a system we refer to as the IRAC system. The purpose of the roadway or link layer controller is to control traffic flow by sending appropriate commands to individual vehicles at the various sections along the highway in addition to ramp metering. The roadway commands include desired speeds to be followed by vehicles at different sections communicated directly to the ACC vehicles for the purpose of harmonizing traffic flow which has beneficial effect on safety and the environment in addition to reducing travel time. The idea of communicating desired speed to manual vehicles includes variable message signs along the freeway. In order to implement the direct communication to ACC vehicles, we propose the use of a dedicated short range communication (DSRC) system. Finally, the IRAC system is evaluated by simulating a freeway traffic network using the microscopic traffic simulation tool VISSIM.

The report is organized as follows: in section 2 we design two roadway control strategies, ramp metering and mainline speed control. In section 3, we introduce the adopted dedicated short range communication system used to communicate speed commands directly to ACC vehicles. In section 4 we construct a simulation model of a freeway stretch along I-80 using the microscopic traffic simulation tool-VISSIM which we validate using field data from the Berkeley Highway Laboratory (BHL). In section 5, we evaluated the proposed IRAC system using different traffic flow scenarios and disturbances in the case of 0% ACC vehicles. In section 6, we repeated the evaluation procedure of section 5 when the penetration of ACC vehicles increases from 0% to 100%. In section 7 we suggest a site for possible deployment of the proposed IRAC system. The conclusions are presented in section 8.

2 INTEGRATED ROADWAY/ADAPTIVE CRUISE CONTROL SYSTEM

The architecture of the proposed IRAC system is shown in Figure 1.

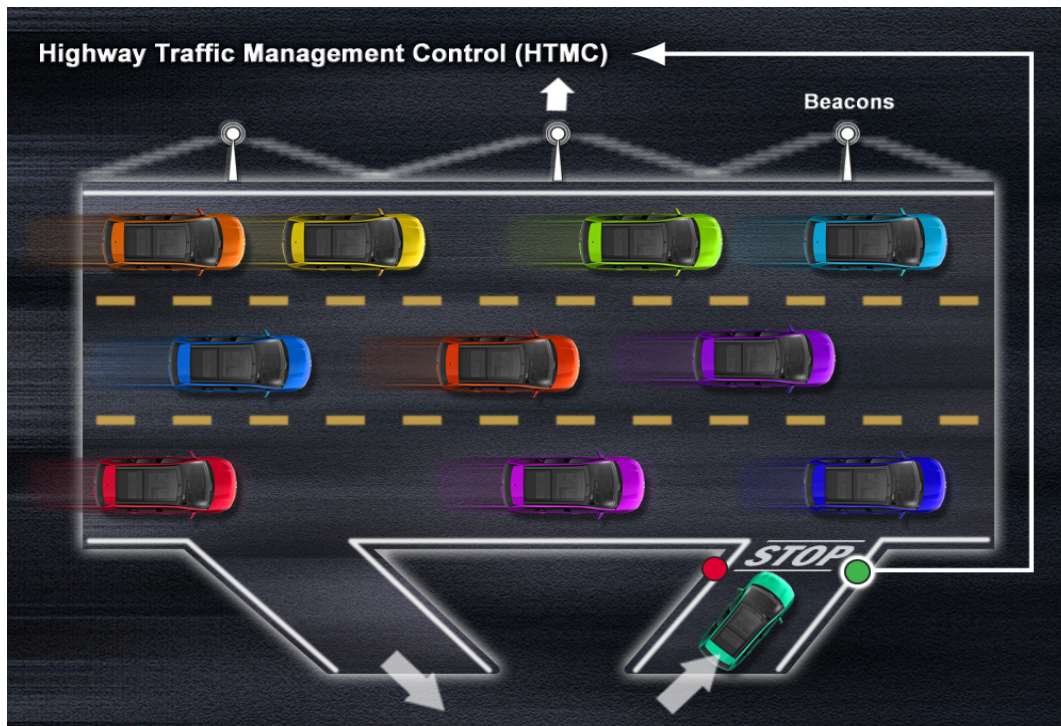


Figure 1: Integrated Roadway/Adaptive Cruise Control (IRAC) System

The highway traffic management center (HTMC) collects information about the status of the traffic and calculates the appropriate commands for the ramps and desired speed limits along the highway lanes. The speed limits are communicated to the individual vehicles via short range vehicle to roadway communications or by bill boards (less advanced system). If the vehicles are equipped with adaptive cruise control systems (ACC), these systems are modified to accept and respond to speed limit commands from the roadway. The non ACC vehicles would have to rely on the human drivers to obey the desired speed limits. Since almost all vehicles are following the vehicles immediately ahead of them, the speed limit commands will be indirectly obeyed by all if at least one driver per each lane obeys the roadway speed limit commands.

The IRAC system can also be viewed as a feedback control system shown in Figure 2.

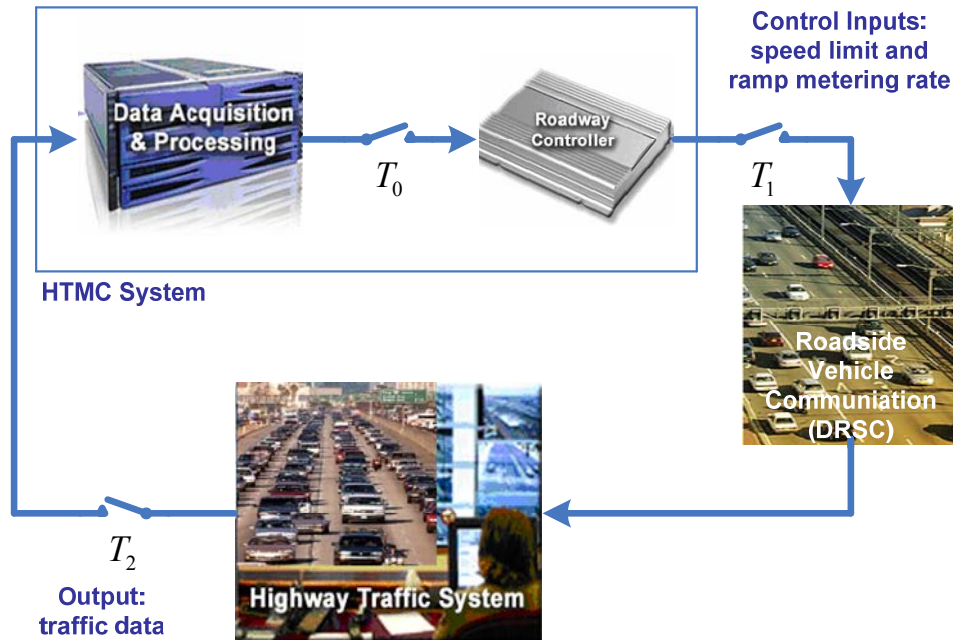


Figure 2: The IRAC as feedback control system

The HTMC system consists of the data acquisition and processing block whose responsibility is to process all traffic measurements obtained at a sampling period T_2 and provide to the roadway controller those measurements which are relevant to control at a sampling rate T_0 . The roadway controller uses these measurements to come up with the control commands which include ramp metering commands and desired speed limits for the various sections of the traffic network. These commands are provided at a sampling period T_1 . In this project we develop roadway control designs and describe how they can be implemented using vehicle to roadway communication. The proposed design is analyzed and evaluated using validated traffic flow simulation models and a stretch of I-80 as a possible implementation site. In the following sections we present the design, analysis, and evaluation of the roadway controller and overall IRAC system.

2.1 System Description and Notation

Consider a freeway stretch which is subdivided into N sections. Each section is about 500m long as shown in Figure 3. Aggregated traffic state variables are collected from traffic surveillance systems or estimated every T_0 seconds, and the controller generates commands every T_1 seconds, where $T_1 = N_c T_0$, N_c is a positive design integer. Once a control command is generated at time nT_1 , it will remain constant during this control interval, i.e. from nT_1 to $(n+1)T_1$. The feedback roadway control system is shown in Figure 2. The freeway stretch and its surveillance system are simulated using the microscopic simulator VISSIM. The notation used is listed below:

T_0 Surveillance system time step size (in this project, $T_0 = 15\text{sec}$)

- T_I Controller time step size ($T_I = N_c T_0$, N_c is a positive integer)
- L_i Length of the i^{th} section
- m_i Number of lanes of the i^{th} section
- $\rho_i(nT_0)$ Aggregated traffic density (in veh/km/lane) of the i^{th} section at time nT_0
- $v_i(nT_0)$ Aggregated space mean speed (in km/h) of the i^{th} section at time nT_0
- $q_i(nT_0)$ Aggregated traffic flow (in veh/h) from i^{th} to $(i+1)^{\text{th}}$ section during time interval $[(n-1)T_0, nT_0]$
- $r_i(nT_0)$ On ramp inflow of the i^{th} section at time nT_0
- $s_i(nT_0)$ Off ramp outflow of the i^{th} section at time nT_0
- $V_i(nT_I)$ Speed limit command of the i^{th} section during time interval $[nT_I, (n+1)T_I]$, ($nT_I = nN_c T_0$)
- $R_j(nT_I)$ Ramp flow command of the j^{th} on ramp during time interval $[nT_I, (n+1)T_I]$, ($nT_I = nN_c T_0$)
- V_{\min}, V_{\max} The lower and upper bounds of speed limits. The upper limit is the default speed limit of the freeway stretch.
- R_{\min}, R_{\max} The lower and upper limits of ramp flow rate
- \mathbf{I}_V The set of the section indices in which speed limits are controlled
- \mathbf{J}_R The set of the section indices in which ramp meters are controlled

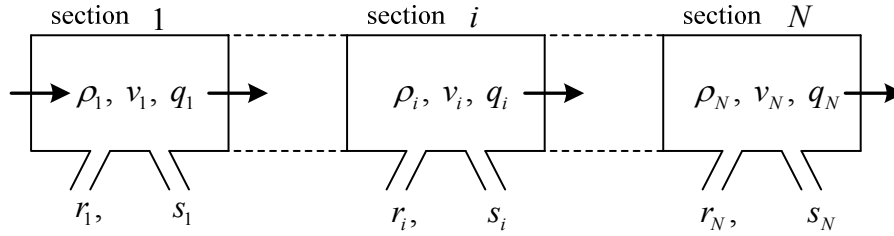


Figure 3: A uni-directional freeway divided into N sections

The above notation and system description are used in the design of the roadway controller in the following sections. The roadway controller consists of two parts: The ramp metering controller and the speed limit controller. We describe each control strategy separately in the following sections.

2.2 Generalized ALINEA Ramp Metering Strategy

Several ramp metering strategies, such as ALINEA, FLOW, METALINE, demand-capacity strategy and occupancy strategy, are investigated in [1, 23]. It has been shown that these strategies are easy to implement and capable of reducing traffic congestion. Since our ramp metering strategy is a modification of ALINEA, we present a brief review of ALINEA. ALINEA is a simple, flexible, robust and efficient local ramp metering strategy. It can be applied without any theoretical pre-investigation or calibration to a broad range of freeway ramps where congestion problems exist. Different studies have

demonstrated that ALINEA is non-inferior to sophisticated coordinated approaches under recurrent traffic congestions [4]. ALINEA can be expressed as

$$R(nT_1) = R((n-1)T_1) + K_r [o_d - o(nT_1)] \quad (2-1)$$

where $R(nT_1)$ is the ramp meter command at time $t = nT_1$, K_r is a control parameter, $o(nT_1)$ is the measured downstream occupancy at time nT_1 , and o_d is the desired value for the downstream occupancy, which is typically chosen close to the critical occupancy o_c [4]. The control strategy described by (2-1) is a simple integral controller where the integral action rejects constant disturbances and reference points in an effort to force the downstream occupancy to stay close to the desired occupancy when the traffic volume is high. In the freeway layout shown in Figure 3, if section j ($j \in \mathbf{J}_R$) contains one on-ramp located near the middle of the section, then a similar ramp metering strategy can be implemented as in (2-1) with the occupancy o replaced by the traffic density ρ_i , and the desired occupancy o_d replaced by the desired density ρ_d . Then, ρ_d can be chosen to be close to the critical density ρ_c in the fundamental diagram. In this project we propose a generalized ALINEA ramp metering strategy, described as follows:

$$R_j(nT_1) = \begin{cases} R_{\max}, & \text{if } \bar{R}_j(nT_1) > R_{\max} \\ R_{\min}, & \text{if } \bar{R}_j(nT_1) < R_{\min} \\ \bar{R}_j(nT_1), & \text{otherwise} \end{cases} \quad (2-2)$$

where

$$\bar{R}_j(nT_1) = R_j((n-1)T_1) + K_r \sum_{m=1}^{N_c} [\rho_d - \rho_j((n-1)N_c T_0 + mT_0)] \quad (2-3)$$

$R_j(nT_1)$ is the ramp command for the ramp on section j at time $t = nT_1$, K_r is a positive controller parameter; ρ_d is the desired density; $j \in \mathbf{J}_R$, \mathbf{J}_R is the set of section indices in which ramp meters are controlled; $T_1 = N_c T_0$, N_c is a positive integer. The ramp metering control strategy is combined with the speed limit control strategy developed in the next section to form the overall roadway controller of the IRAC system.

2.3 Speed Limit Control Strategy

The current highway traffic is operating as an almost open loop dynamical system. Ramp metering provides some feedback by controlling the volume of vehicles entering the highway through the ramps but there is no control of the vehicles coming into the highway network with different speeds from different branches of the highway. A small traffic disturbance due to short duration accident or vehicle break down creates a shock wave that takes long time to be dissipated due to the fact that vehicles away from the

accident could be at high speeds where vehicles close to the accident are at almost zero speed. This possible high speed differential along the highway lanes is also associated with a high differential in the traffic density. It results to low speed, high density waves which propagate upstream and persist for much longer time than it takes to clear the accident or the vehicle break down. One way to close the loop to this physically unstable dynamical system is to calculate the desired speeds vehicles need to follow at each section of the highway for a given traffic flow situation and communicate them to the vehicles using variable message signs along the freeway [12] or via short range roadway to vehicle communication. It has already been shown that the use of variable speed limits have the potential of improving traffic performance [12, 14, 15] if properly designed. It has also been demonstrated that the coordinated control of variable speed limits and ramp metering increases the range in which ramp metering is useful [16]. The deployment of roadway control systems involving variable speed limits is feasible with current communication technologies as discussed in section 3. Various speed control strategies have been proposed in the literature [14-17] based on some second order traffic flow models. These control strategies usually are computationally intense, and their robustness is questionable since the design models involve many unknown parameters which have to be estimated or calibrated apriori. In this project we propose a simple speed control strategy based on information from the fundamental flow-density relationship as follows:

Denote C_i ($i \in \mathbf{I}_V$) as the controller generating the desired speed limit \bar{V}_i for section i . The following switching rules are used to determine whether C_i should be active or not:

- S1.** If $\rho_{i+1}(nT_1) \geq (1 + \Delta_+) \rho_c$, where Δ_+ is a positive design parameter and ρ_c is the critical density, then C_i is active.
- S2.** If $\rho_{i+1}(nT_1) \leq (1 - \Delta_-) \rho_c$, where Δ_- is a positive design parameter, then C_i is inactive.
- S3.** Otherwise, C_i maintains at the same status as in the previous control time interval.

The above rules prevent frequent switches of the controller between the active mode and the inactive mode. The speed of the traffic flow at each section i satisfies an upper and lower bound

$$V_{\min} \leq V_i(nT_1) \leq V_{\max} \quad (2-4)$$

where V_{\min}, V_{\max} are positive constants. When C_i is inactive, the desired speed limit is the default speed limit of the i -th freeway section.

When C_i is active, section i is regarded as a virtual on ramp of section $i+1$ and the same generalized ALINEA ramp metering strategy is applied to regulate the flow rate Q_i from section i to section $i+1$, i. e.

$$Q_i(nT_1) = \begin{cases} Q_{\max}, & \text{if } \bar{Q}_i(nT_1) > Q_{\max} \\ Q_{\min}, & \text{if } \bar{Q}_i(nT_1) < Q_{\min} \\ \bar{Q}_i(nT_1), & \text{otherwise} \end{cases} \quad (2-5)$$

where,

$$\bar{Q}_i(nT_1) = Q_i((n-1)T_1) + K_v \sum_{m=1}^{N_c} [\rho_d - \rho_{i+1}((n-1)N_c T_0 + mT_0)] \quad (2-6)$$

and K_v is a controller parameter. ρ_d is the desired density; $i \in \mathbf{I}_V$, \mathbf{I}_V is the set of section indices in which speed limits are controlled; $T_1 = N_c T_0$, N_c is a positive integer. The above equations however provide the regulation of the flow at a particular section of the highway. Our control variable however is speed. Therefore in order to regulate traffic speed instead of the traffic flow rate as done in ramp metering, we use the flow rate to speed relationship as described by the fundamental flow-density diagram, shown in Figure 4. We set Q_{\max} as the flow corresponding to the critical density, which is the capacity. We denote by v_c the speed corresponding to the critical density. It is reasonable to assume that $V_{\min} \leq v_c \leq V_{\max}$. Therefore, we could set Q_{\min} as the flow corresponding to V_{\min} . A mapping from $[Q_{\min}, Q_{\max}]$ to $[V_{\min}, v_c]$ could be found, denoted as $f(Q)$. The flow-density relationship of every section could be estimated either offline or online [24]. Therefore, the mapping $f(Q)$ is defined based on the estimated flow-density relationship. Specifically, if the flow-density relationship is assumed to be:

$$q = \rho \cdot v_f \cdot \exp \left[-\frac{1}{\alpha} \left(\frac{\rho}{\rho_c} \right)^\alpha \right] \quad (2-7)$$

then the free flow v_f , critical density ρ_c , and the exponent α , could be estimated online or offline using real traffic data and used to find the mapping $f(Q)$, as shown in Figure 5.

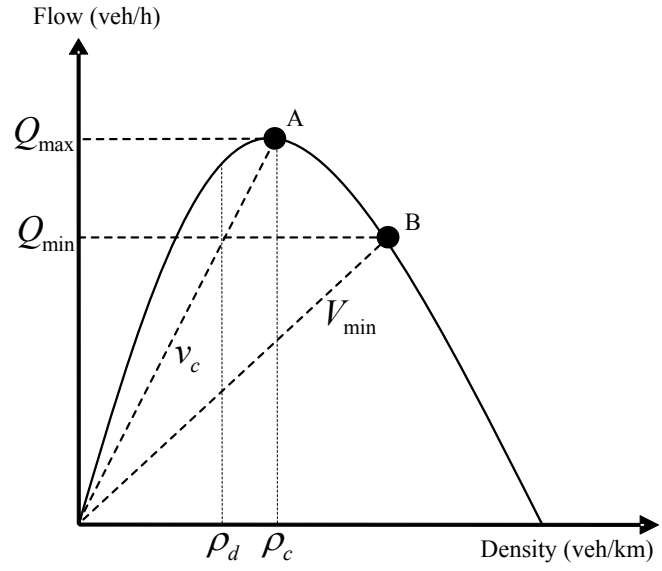


Figure 4: Fundamental flow-density diagram

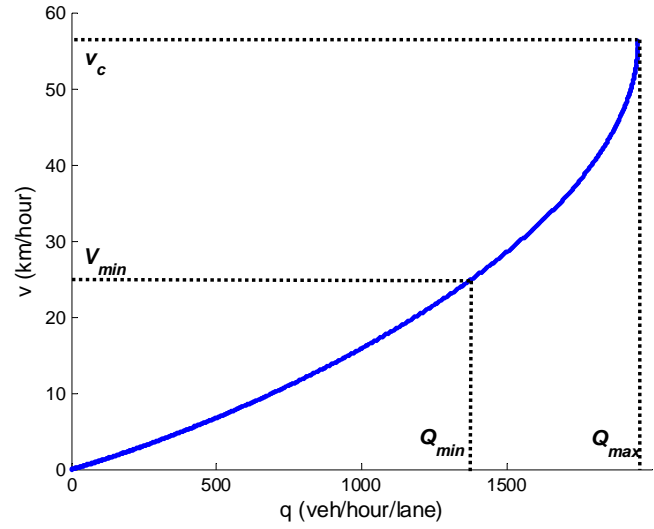


Figure 5: $f(Q)$, strictly increasing mapping from $[Q_{min}, Q_{max}]$ to $[V_{min}, v_c]$

Therefore, when C_i is active, we have the desired speed limit as:

$$\bar{V}_i(nT_1) = f(Q_i(nT_1)) \tag{2-8}$$

However, \bar{V}_i generated by (2-8) may lead to unsafe changes of speed limits. For practical purposes, we use the following speed limit V_i which is smoother:

$$V_i(nT_1) = \begin{cases} V_i((n-1)T_1) - c_v, & \\ \quad \text{if } \bar{V}_i(nT_1) \leq V_i((n-1)T_1) - c_v, & \\ V_{i+1}(nT_1) + c_v, & \\ \quad \text{if } \bar{V}_i(nT_1) \geq V_{i+1}(nT_1) + c_v, & \\ \bar{V}_i(nT_1), \text{ otherwise} & \end{cases} \quad (2-9)$$

where c_v is a design constant.

If C_i is inactive at time $(n-1)T_1$ and becomes active at time nT_1 , the speed limit is given as:

$$V_i(nT_1) = \begin{cases} V_{i+1}(nT_1) + c_v, & \\ \quad \text{if } \bar{V}_i(nT_1) \geq V_{i+1}(nT_1) + c_v, & \\ \bar{V}_i(nT_1) = f(\rho_{i+1}(nT_1)v_{i+1}(nT_1)), \text{ otherwise} & \end{cases} \quad (2-10)$$

The roadway controller of the overall IRAC system consists of the ramp metering strategy given by (2-2) and the speed control strategy given by (2-9, 2-10) and rules **S1-S3**. In the following subsection we present a communication approach how to communicate the desired speed limits to individual vehicles.

3 ROADWAY TO VEHICLE COMMUNICATION

The rapid evolution of wireless communication technologies provides opportunities to utilize these technologies in support of traffic flow control. The U.S. Department of Transportation proposed the system architecture for the development of Intelligent Transportation Systems (ITS), shown in Figure 6 [25]. The new Dedicated Short Range Communication (DSRC) at 5.9 GHz was proposed to be used for Roadway to vehicle (r2v) communication and vehicle to vehicle (v2v) communication. The corresponding standards have been developed, such as ASTM E2213-03 (Standard Specification for Telecommunications and Information Exchange between Roadside and Vehicle Systems — 5 GHz Band Dedicated Short Range Communications (DSRC) Medium Access Control (MAC) and Physical Layer (PHY) Specifications) in North America. Similar standards have been developed by the European Union and Japan. ASTM E2213-03 is aiming to provide wireless communication capabilities for transportation applications within a 1000-meter range at typical highway speeds, with communication rates up to 27Mbps. It provides seven channels at the 5.9 GHz licensed band, each covering a 10-MHz band, as illustrated in Figure 7 [26]. One channel is set especially for control applications (Channel 178).

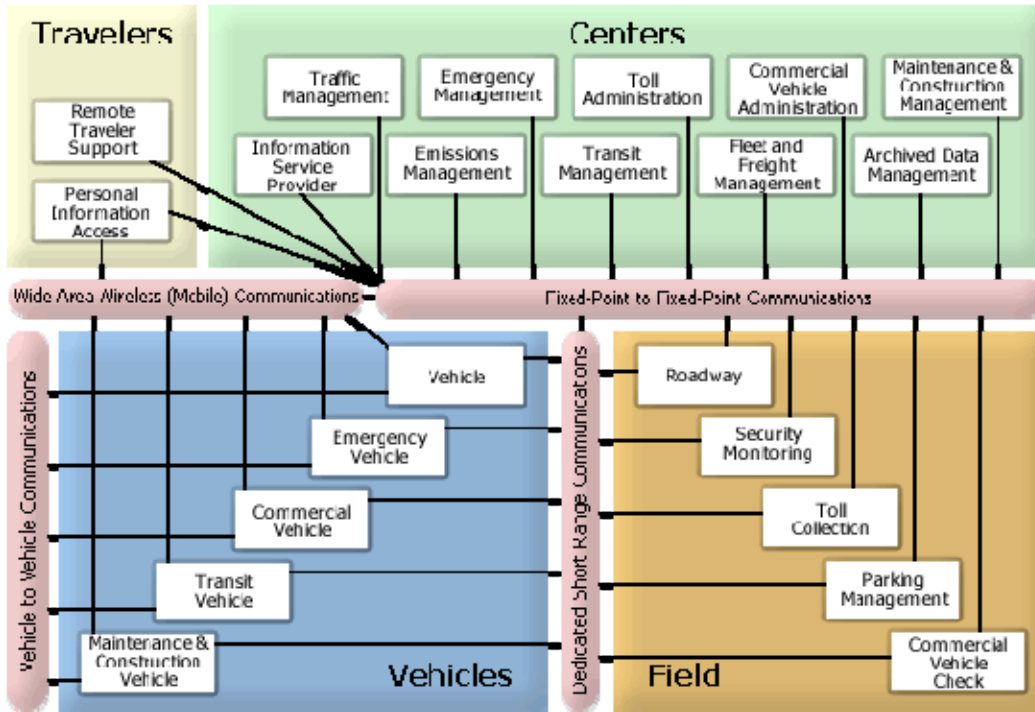


Figure 6: ITS Architecture

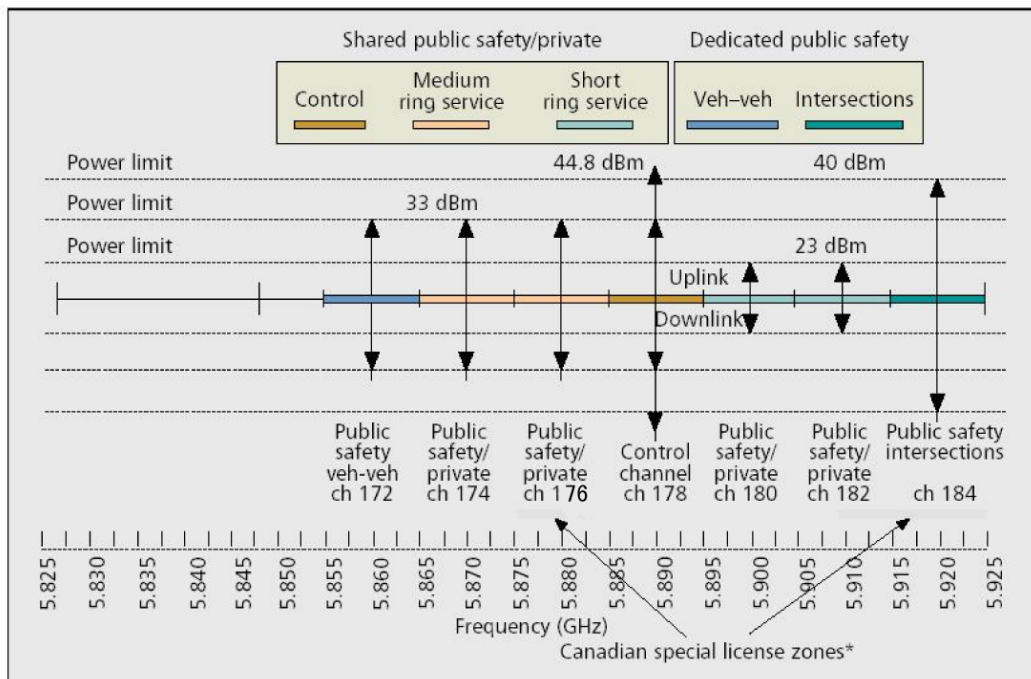


Figure 7: 5.9 GHz DSRC band plan with 10 MHz channels and power limit

Based on the DSRC standards, we propose a roadway to vehicle (r2v) communication system to facilitate speed limit communication to ACC and manual vehicles, as illustrated in Figure 8. The system is composed of three parts: on-board unit (OBU), road-side unit (RSU) and remote highway traffic management center (HTMC). The speed limit control algorithm proposed in this report is based on a segmented freeway topology (Figure 3) with sections about 500 m long. In the beginning of every section, a RSU is installed on the side of the freeway and broadcasts the current speed limit to the vehicles in its communication zone. The communication zone of every RSU is about 100m long and covers all the lanes in one direction. The real time speed limit for every section is assigned by HTMC via wide area network. The proposed r2v system consists of three layers: physical layer, data link layer (MAC and logic link control) and application layer. Figure 9 shows the suggested system architecture by IEEE Std 1455-1999 (IEEE Standard for Message Sets for Vehicle/Roadside Communications).

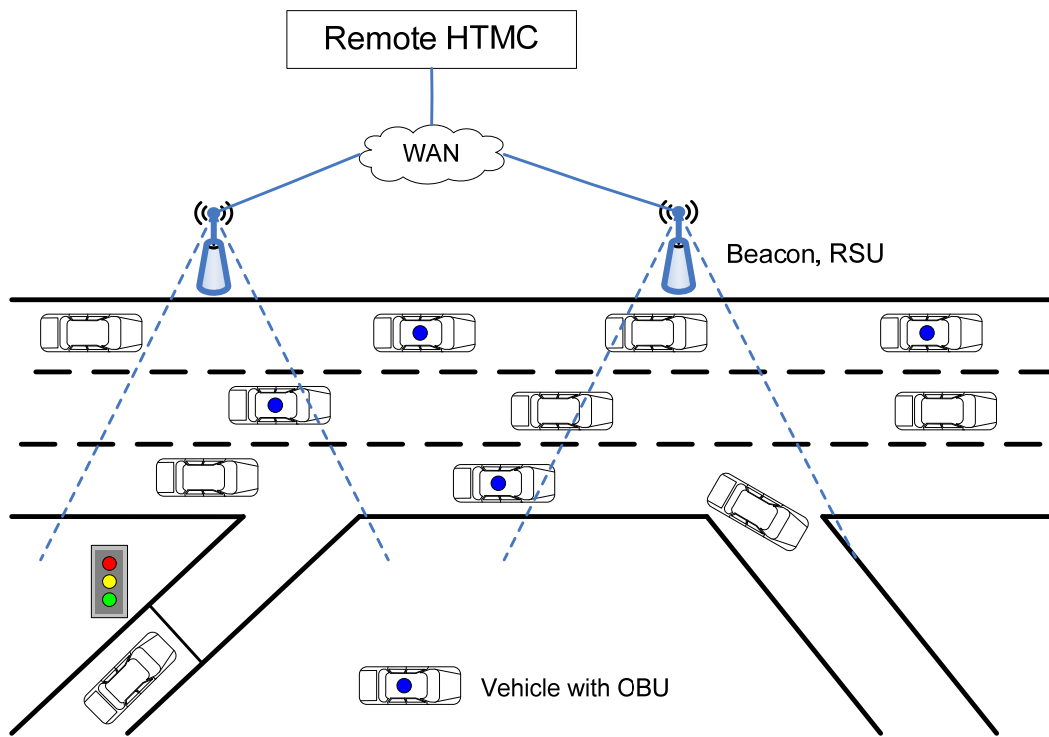


Figure 8: Roadside to vehicle communication system

For the application (speed limit control) proposed in this report, the DSRC communication system is required to have the following characteristics: [27]

1. Transmission from roadside infrastructure to vehicles.
2. One-way communication.
3. Point-to-multipoint communication.
4. Transmission mode: periodic
5. Minimum frequency: more than 1Hz.
6. Allowable latency: about 1 second, (the control interval T_l is 1 min in this report).
7. Data to be transmitted: real time speed limit.
8. Maximum required range of communication: 100m

To justify some of the above requirements, assume the worst case scenario: a car passing the communication zone at 85mph. The time it needs to travel the 100m communication zone is about 2.6s. During this 2.6s, speed limit information is broadcasted at least twice. RSU and OBU that are manufactured following DSRC standard ASTM E2213-03 will be able to meet all the requirements above.

For the application layer protocols, the one that is suitable for Electronic Toll Collection (ETC) system is applicable to the speed limit roadway to vehicle communication presented in this report. Indeed, only the broadcast mode is needed. Examples of such standards are ISO 14906:2004 (Road transport and traffic telematics -- Electronic fee collection -- Application interface definition for dedicated short-range communication) and IEEE Std 1455-1999 (IEEE Standard for Message Sets for Vehicle/Roadside Communications).

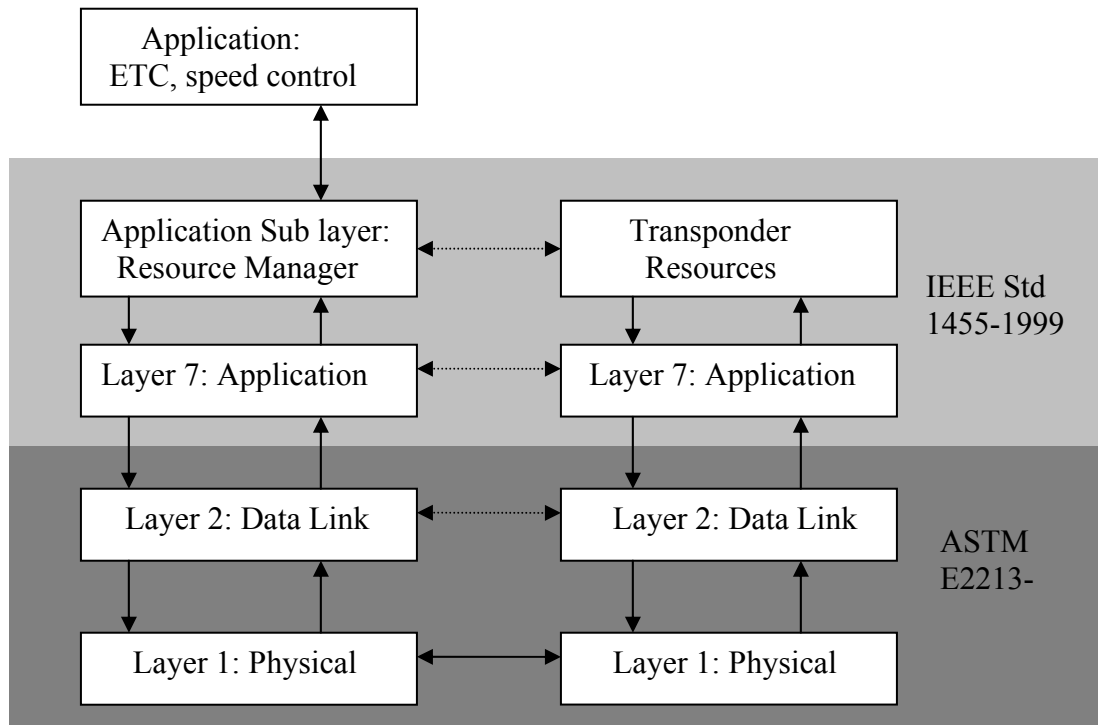


Figure 9: DSRC system architecture

It is therefore clear that the implementation of the communication component of the IRAC system can be easily done using existing technology and approved frequency bands and communication protocols.

4 MICROSCOPIC SIMULATION MODELING AND VALIDATION

Since actual experiments involving new traffic flow control algorithms are not desirable due to cost and possible adverse effects on traffic, extensive simulation studies need to be performed to evaluate the performance and robustness of the proposed IRAC system before an actual demonstration.

Simulation models could assist transportation engineers in evaluating alternative transportation strategies and in predicting outcomes of an improvement of the transportation systems. Traffic simulation models can generally be classified into macroscopic, mesoscopic and microscopic models. Macroscopic simulation models are usually based on deterministic relationships of flow, speed, and density of the traffic stream. Mesoscopic models are also based on macro flow dynamics. Microscopic models simulate the individual vehicle movements based on car-following and lane-changing theories and are usually stochastic [28].

Although macroscopic models need less computing power and calibrating efforts, it is sometimes not sufficient to capture the desired level of details of a transportation system. On the other hand, microscopic models have increased their area of application since more computing power is available. Accordingly, microscopic models are effective in the operation of complex transportation systems and the investigation of ITS (Intelligent Transportation System) where greater levels of details are required. However, those models require a great deal of computational effort and calibration since there are numerous parameters which affect the traffic flow and need to be calibrated. Modern traffic surveillance systems provide us field data from loop detectors, video cameras, microwave sensors, probe vehicles, and other detection methods. Since most of the microscopic models are based on car-following models, vehicle spacing information extracted from measured field data can be used for the calibration of car-following models.

The Federal Highway Administration (FHWA) developed and maintained CORSIM which stands for CORridor SIMulation which evolved from two separate traffic simulation programs NETSIM and FRESIM. NETSIM models arterials with signalized and unsignalized intersections, while FRESIM models uninterrupted freeways and urban highways. CORSIM has been used extensively for traffic flow simulations and analysis. During the last decade several commercial traffic flow simulators have been developed which include VISSIM, AIMSUN, and PARAMICS as the most publicized ones giving users a wide range of choices and software tools for generating microscopic simulation models of traffic networks. In this project we initially used CORSIM and then switched to VISSIM after we learned that FHWA may discontinue its maintenance of CORSIM. In addition VISSIM appeared to have certain capabilities that made it easier to simulate the IRAC system.

In this project, a stretch of the Interstate-80, immediately east of the San Francisco-Oakland Bay Bridge associated with the Berkeley Highway Laboratory (BHL) is simulated using a microscopic simulation model. Measured data are used to tune and

calibrate the model so that it accurately represents the traffic flow characteristics. Since the measured data were available for only part of the highway the model was extended to include several more ramps in its downstream assuming that its behavior will not change. This extended freeway model is used to analyze the performance of the proposed IRAC system for different levels of penetration of ACC vehicles. The results of these simulation studies are presented in the following sections.

4.1 Freeway Model and Field Data

4.1.1 Freeway Model

The Berkeley Highway Laboratory (BHL) is chosen as the site for data collection and simulation model validation since there is a detailed description of the site accompanied with comprehensive traffic data which are readily available. The BHL is a test site covering 2.7 miles of the Interstate-80 immediately east of the San Francisco-Oakland Bay Bridge. The facility provides traffic data collected by sixteen directional dual-inductive-loop-detector stations [29].

The unidirectional freeway stretch used for this study is constructed from northbound lanes of the BHL site. BHL mainline has five lanes including one HOV (High Occupancy Vehicle) lane. However, the existence of HOV lanes was not considered here because this study intends to validate the aggregated flow from five lanes and to control the corresponding traffic. Also, the freeway curvature was not considered since the degree of curvature in the area is not high enough to affect the traffic. In order to estimate the flow rates of the on-ramps and off-ramps, the data set from seven detector stations are used for validation of the simulation model. The freeway stretch includes two on-ramps (Ashby Ave. and University Ave.) and one off-ramp (University Ave.). Figure 10 shows the layout of the extended BHL. The triangular marks represent the data collection stations of BHL. That is, only the upper part of the layout is considered in the validation phase.

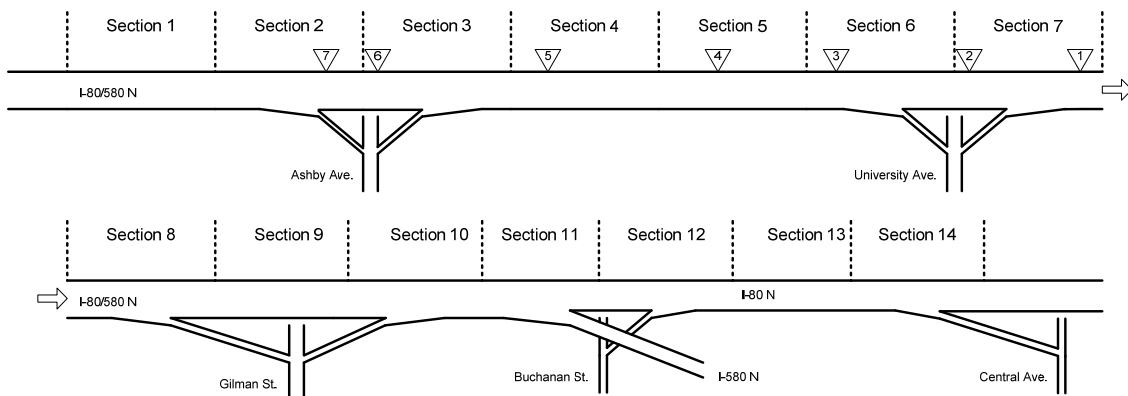


Figure 10: Layout of the extended BHL

4.1.2 Field Data

The field data consisting of 30-second summary data files were downloaded from the BHL website. Specifically, data from four different days of June 2004 were selected. The data showed a similar congestion pattern, i.e., duration of the congestion, peak flow rate, and congested speed. The downloaded data sets have a sampling period of 30 seconds, including aggregated flow and traffic speed measurements. Since our simulation period is 12 hours (from 10am to 10pm), we increased the sampling period to 5min. 5min data reduce the computational load of the simulator and make the estimation of the ramp flows easier. Using this 5min data, ramp flows are estimated by subtracting flows of two mainline detectors before and after the corresponding ramp.

4.2 Construction of Freeway Model using VISSIM

Microscopic simulation tools are more sophisticated than before due to the availability of more powerful computers and software tools and are frequently used in traffic analysis. These tools, such as CORSIM [30] and VISSIM [31], are designed to model any combination of surface transportation networks at a high level of detail. They support different signal control and other operational strategies and provide various output formats for analysis and comparison. The properties of several popular microscopic simulation models have been investigated in [32, 33, 34].

4.2.1 Introduction of VISSIM

In our earlier work the traffic network under consideration was simulated using CORSIM [17], a software package developed and supported by FHWA. Due to some limitations of CORSIM and discussions of possible termination of support we switched to VISSIM which is a commercial package. A quantitative comparison of the simulation models based on VISSIM and CORSIM, indicated that the two models perform very similar. The two software packages however differ in their network coding structures, signal modeling logic, car-following models, and etc. CORSIM uses a link-node representation to build a network, while VISSIM uses link-connector structure which can be constructed over an imported graphical map. It is known that this unique network coding structure enables VISSIM to model any kind of intersection or any length of link. Also, the structure makes it possible to divide the freeway into subsections with little effort. Due to its flexibility, VISSIM is selected to simulate various needs in the field of traffic analysis [35, 36, 37]. VISSIM is a discrete, stochastic, time step based microscopic traffic simulation program developed to analyze traffic and transit operations. VISSIM uses the psycho-physical driver behavior model based on the continued work of Wiedemann [38, 39]. The basic idea of this model is stochastic perceptual thresholds which replicates individual driver characteristics.

4.2.2 Construction of the Freeway Stretch in VISSIM

Coding of the Network

The sources of geometric information about the selected network were detailed drawing of BHL accessible from BHL website and scaled aerial photographs accessible from Google Maps (<http://maps.google.com/>). Several network entities are placed over the constructed freeway stretch based on the sources. A set of *Detectors* are placed to model each BHL data collection station. A set of *Desired Speed Decisions* is also installed right before the corresponding station and is activated during some initialization period of each simulation run. *Reduced Speed Area* is placed right before *Signal Head* to generate more realistic traffic behavior on the curved area of a ramp.

Coding of the Ramps

As described in the manual, on-ramps are configured by adding merging lanes on the mainline and by placing appropriate *Routing Decisions*. However, this approach generates unrealistic behaviors (a large queue on the on-ramp while fast through traffic in merging area) as the mainline flow approaches its critical density. These problems can be addressed by *Direction Decision*. By diverting a percentage of vehicles on one or two rightmost lanes to other lanes, it allows space for the on-ramp flow to merge into the mainline. However, it may cause other unrealistic behaviors in its downstream when the next *Connector* is rather far or the next ramp is close to the current one because it may increase the flow on the leftmost lanes of the mainline. The *Reduced Speed Area* and *Lane Change* distance on *Connector* can be used to address these unrealistic behaviors. By placing the *Reduced Speed Area* right before the merging area and by increasing the *Lane Change* distance on the *Connector* after the merging area, it prevents vehicles on the mainline from using the merge lane as an acceleration lane as well as make sure that the vehicles on the ramp are aware that they do need to merge before this *Connector*.

Similar to the on-ramp configuration, off-ramps are modeled by adding splitting lane on the mainline. Off-ramp flow can be defined by the *Direction Decision* or *Routing Decision*. The *Routing Decision* accompanied by proper *Reduced Speed Area* and *Lane Change Distance* is also chosen to generate more realistic behaviors.

For both kinds of ramps, the range of the *Routing Decision* is defined to be wide enough to capture the behavior of the upstream traffic as long as the geometry allows. Also, the *Lane Change* distance is set to be greater than the default value in order to generate a visually acceptable lane changing behaviors.

Coding of the Signal Control

In VISSIM, ramp metering can be modeled either using the built-in fixed-time control or an optional external signal state generator. Metered on-ramps in the field are usually operated by traffic-responsive control. The operation time of a metered on-ramp varies from place to place. Also, it may follow the platoon metering or not. Therefore, for

simplicity, the validation of the simulation model assumes that all ramp meters follow a fixed-time control. The fixed cycle for signals is set to provide the basic saturation flow indicated by the Highway Capacity Manual (HCM). It is generally accepted that a saturation flow rate of 1,800 vehicles per hour per lane is a realistic average under ideal conditions [40]. Since fixed-time control is applied to this validation part, the built-in signal controller inside the simulator is suitable for the validation phase. However, an external signal state generator is chosen for the control logic since the validated highway simulation model will be used to evaluate complicated ITS strategies (e.g. advanced ramp metering, variable speed control, and etc.).

Traffic actuated signal controls can be simulated in VISSIM by the external signal state generator (VAP or other external program). VAP (Vehicle Actuated Programming) is an optional add-on module of VISSIM for the simulation of programmable, phase or stage based, traffic actuated signal controls. This module is programmable with a simple descriptive language. It receives detector variables, interprets control logics, and creates signal commands on a discrete time step basis. However, it is incapable of generating variable speed commands and it is not sufficient to perform complex mathematical computations. Therefore, an external Dynamic Link Library (DLL) is added as the signal state generator. The DLL interface package was acquired from VISSMI Hotline and modified to fit our purposes. It can access the VISSIM kernel functions to create signal and speed commands during a simulation run. A communication function with MATLAB is added in order to perform a proposed strategy which requires a higher level of mathematical computations. Using this interface, any complex form of controller can be applied to our IRAC system while a relatively simple controller is currently implemented. MATLAB provides interfaces to external routines written in other programming languages, data that needs to be shared with external routines, clients or servers communicating via Component Object Model (COM) or Dynamic Data Exchange (DDE), and peripheral devices that communicate directly with MATLAB [41].

Coding of the Traffic Composition

VISSIM uses a hierarchical concept to define the vehicle population. *Vehicle Types* defines a group of vehicles that have similar characteristics, such as, *Vehicle Model*, *Length*, *Width*, *Maximum (Desired) Acceleration*, *Maximum (Desired) Deceleration*, etc. Some of these characteristics are defined with probabilistic distributions in VISSIM. Also, *Vehicle Class* is used to aggregate one or more *Vehicle Types* which have a similar driving behavior. The following vehicle types are defined for our purposes: CAR (manual passenger vehicles) and ACC (ACC-equipped passenger vehicles). This can be done by using *Links Types* and *Traffic Compositions*. Therefore, only CAR is used in the validation phase.

Coding of the Traffic Demands

As a Windows application, VISSIM provides a window for editing each network entity or decision. Since the time interval for the validation is set to 5min, a great amount of effort is required to manually edit the inputs, especially for *Vehicle Inputs*, *Desired Speed*

Decisions, and Routing Decisions. Therefore, a MATLAB program Input Generator (InpGen.m) is developed to directly edit the VISSIM network file. InpGen extracts speed and flow information from BHL data and converts them into 5min format. Based on the 5 min data, each input for the corresponding period is written in the VISSIM network file with its appropriate text structure.

System Architecture

The validation process requires multiple simulations with different random seeds over several sets of data. An external C program (MultiRun) which executes COM commands is developed to run a VISSIM model with different random seeds or to run several models sequentially. COM interface provides access to model data and simulation objects, which allows VISSIM to work as an Automation Server and to export the objects [42]. The system architecture for the simulations is shown in Figure 11. The communication functions represented by the dotted lines are not used for this validation phase, but they are prepared for the simulations with the IRAC system.

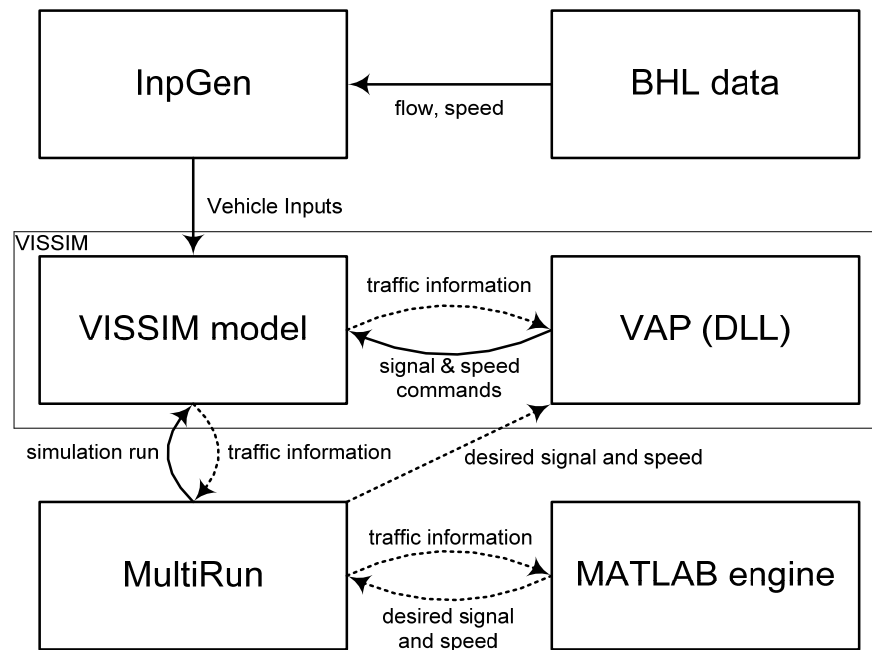


Figure 11: System architecture for the simulations

4.3 Model Validation Results

4.3.1 Estimation and Calibration of Parameters

The traffic flow model in VISSIM is a discrete, stochastic, time step based, microscopic model. The model contains a psycho-physical car following model for longitudinal vehicle movement based on the Wiedemann 1999 car following model. Several parameters involved in this model are quite sensitive and need to be calibrated. These parameters could be expressed in the following equation:

$$s = CC0 + CC1 \cdot v + l + CC2/2 \quad (4-1)$$

where $CC0$ is the standstill distance, $CC1$ is the headway time, l is the vehicle length, $CC2$ is the car following distance variation, v is vehicle speed and s is the spacing.

Due to the fact that spacing s is approximately the inverse of density ρ , and that we could estimate the relationship between ρ and v in steady state, our first guess of these parameters came from the estimation of the following two parameters : h and d , in equation (4-2):

$$s = h \cdot v + d = 1.4934 \cdot v + 9.2099 \quad (4-2)$$

where h , the time headway, and d , the intervehicle spacing at zero speed, are estimated by least squares estimation using 4 days of BHL field data. Flow and speed measurements in the free flow region of these 4 days data were pooled together. Spacing estimates were obtained by using $s = v/q$. As shown in Figure 12, blue points are points (spacing, speed) from field data; red points are the fitted straight line by least square estimation. Therefore, the slope of the line is approximately the time headway h and the intercept of the line is approximately the parameter d . Comparing (4-1) and (4-2), we could get nominal values for $CC1$, which is around 1.5, and $CC0 + l + CC2/2$, which is around 9. Consider the common length of a car (including the standstill distance) to be around 6 meters, then $CC2/2$ is around 3, i.e., $CC2$ is around 6.

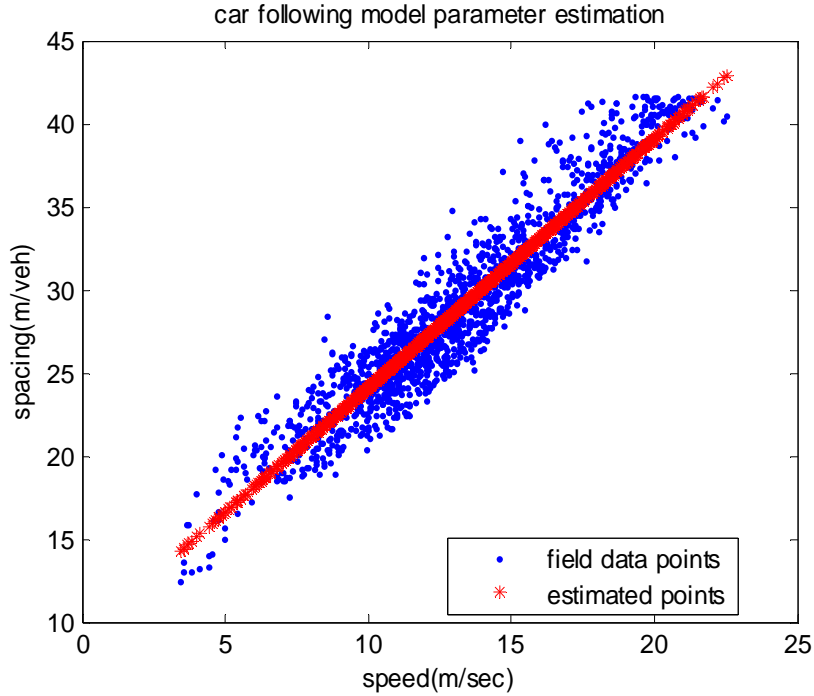
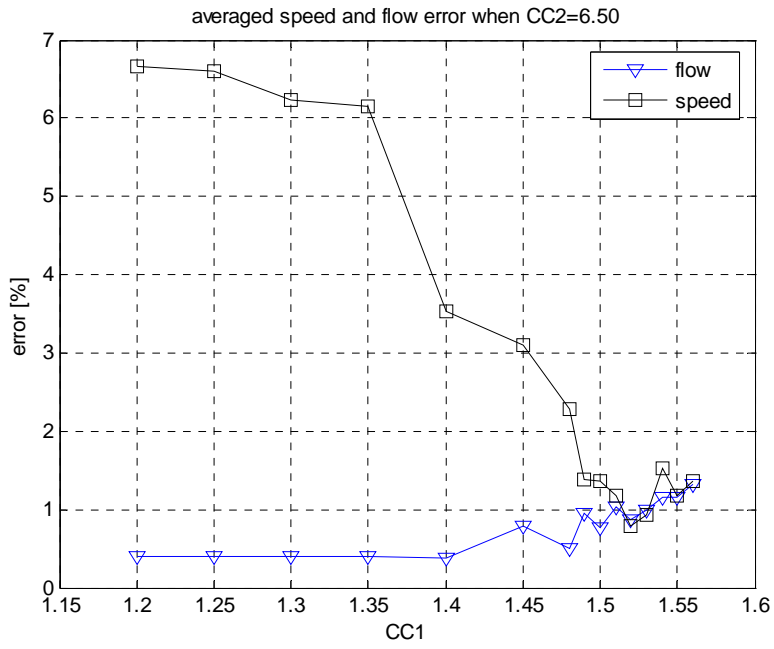


Figure 12: Car following model parameter estimation using field data.

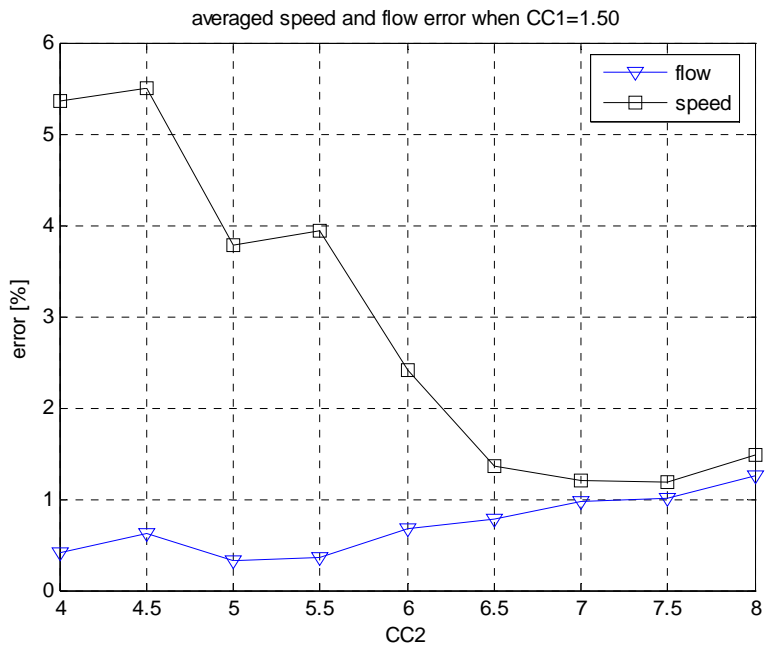
The purpose of this validation is to construct a simulation model which accurately describes the traffic flow characteristics and then use it to evaluate our proposed IRAC system. Since CC1 and CC2 have a major influence on the safety distance and the capacity, we calibrated these two parameters using multiple simulation runs while varying one of the two parameters and fixing the other parameters around their nominal values. The errors between the field and the simulated data of these simulation runs are investigated. In Figure 13(a), CC2 is fixed at 6.50 and CC1 is varying from 1.2 to 1.6. The percentage error of speed and the percentage error of flow were plotted against the parameter CC1 with different symbols. The plots show that the speed error decreases as CC1 goes to 1.5 and stays afterwards and that the flow error does not have many fluctuations as CC1 varies. In Figure 13(b), CC1 is fixed at 1.50 and CC2 varies from 4 to 8. Similarly, the speed error decreases as CC2 goes to 6.5 and stays afterwards while at the same time the flow error fluctuates little as CC2 varies. Therefore, in an effort to keep the discrepancy small the parameters are chosen as CC1=1.5, CC2=6.5. The percentage error of speed is defined as

$$\left| \frac{\text{average simulated speed} - \text{average field speed}}{\text{average field speed}} \right| \times 100\%$$

where the speeds are averaged over all the sampled measurements and the percentage error of flow is defined similarly.



(a)



(b)

Figure 13: Parameter sensitivity with respect to speed and flow errors

4.3.2 Comparison of Field Data and Simulated Data

Figures 14, 15 show the validated results from one of the four days. The data plotted are flow measurements (Figure 14) and speed measurements (Figure 15) from 7 loop detector stations on BHL sampled every 5mins for 12hours. Figure 14 and 15 are both 3-D mesh plots with time (in hours) and distance (in station number) as X and Y axes, and with flow (in veh/hour/lane) or speed (in km/h) as Z axes. By comparison of the flow measurements from field data and the flow measurements from simulation runs with calibrated parameters in Figure 14 and the field velocity measurements and the simulated velocity measurements in Figure 15, we can see that the model properly captures the congestion characteristics of the BHL section. Figure 16 shows the speed-flow relationship of the same field data and simulated data as in Figure 14&15. Data points shown in Figure 16 are pooled from all the stations together. The capacity estimated from Figure 16(a) and (b) are both around 1900 veh/h/lane.

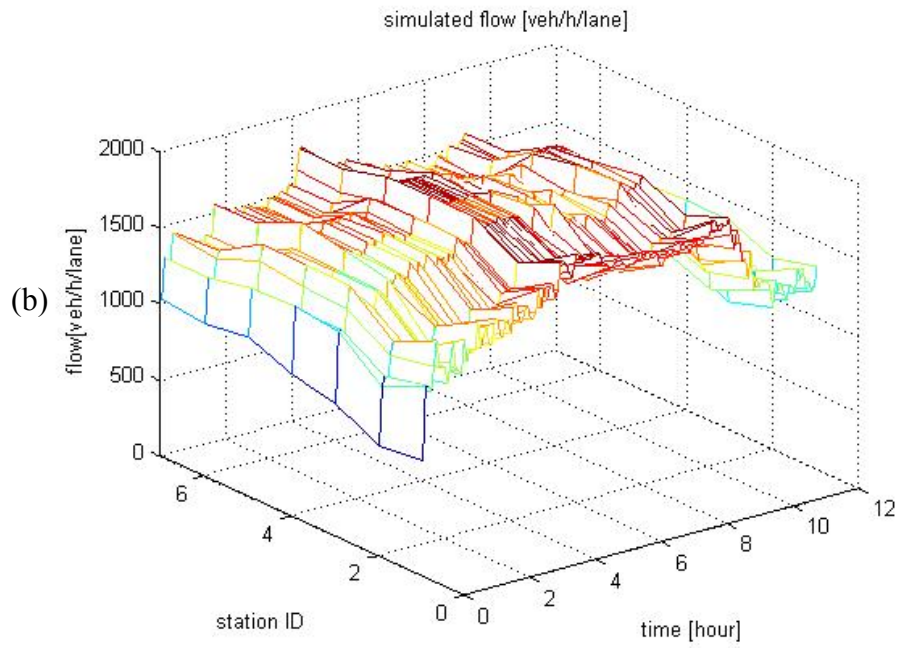
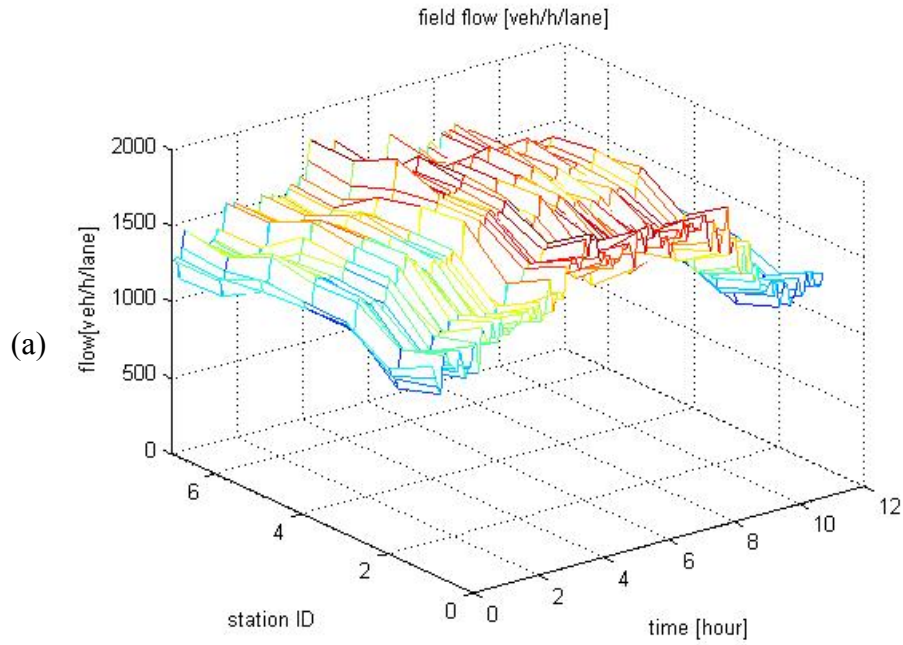


Figure 14: (a) Field flow (b) Simulated flow

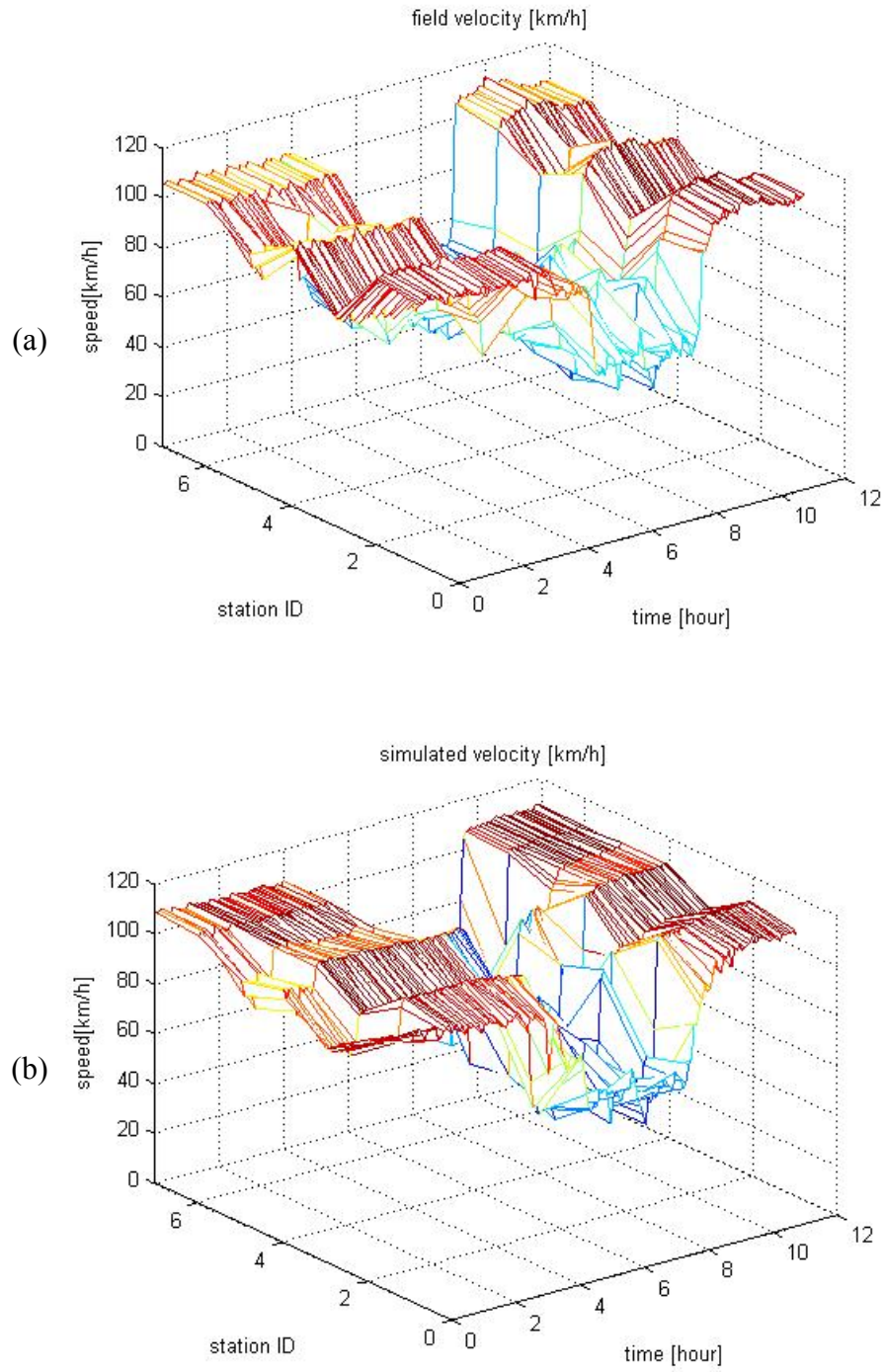


Figure 15: (a) Field velocity (b) Simulated velocity

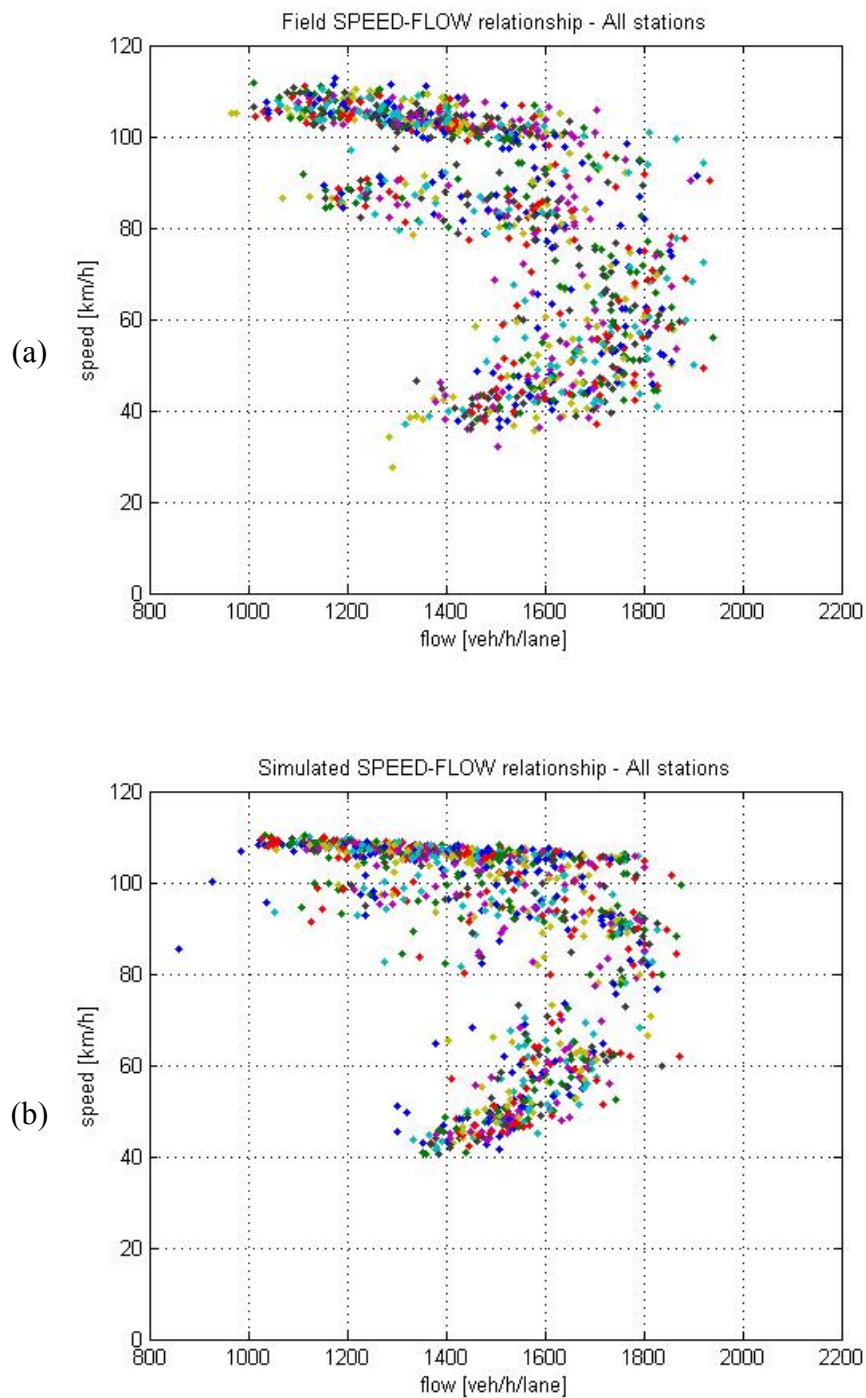


Figure 16: (a) Field speed-flow relationship (b) Simulated speed-flow relationship

The above figures demonstrate that the tuned simulation model represents rather accurately the traffic flow characteristics and can therefore be used for studying hypothetical scenarios of implementation of the IRAC system.

5 DEPLOYMENT SCENARIOS AND EVALUATION

5.1 Traffic Scenarios

Freeway congestion is generally caused by recurrent bottlenecks during peak hours and non-recurrent bottlenecks such as accidents, events, weather changes and etc. The proposed IRAC system is evaluated using the validated microscopic model for different congestion scenarios. The index set for ramp metering is $\mathbf{J}_R = \{3, 7, 12\}$, and the set for speed control is $\mathbf{I}_V = \{i | 4 \leq i \leq 11\}$. The on-ramp or off-ramp flow rates are modeled using the simple assumptions:

$$r_i(nT_0) = \beta_i q_{i-1}(nT_0) \quad (5-1)$$

$$s_i(nT_0) = \beta_i q_{i-1}(nT_0) \quad (5-2)$$

where β_i is a non-negative constant and it is zero when there are no ramps for section i . Table 1 shows the status of ramp controllers and mainline controllers. Freeway I-580 is treated as an off-ramp on section 11 with a higher outflow rate. Table 2 shows the values of the controller parameters used in the simulations.

Section#	1	2	3	4	5	6	7	8	9	10	11	12	13	14
On Ramp β_i	0	0	0.1	0	0	0	0.1	0	0	0.1	0	0.1	0	0
Off Ramp β_i	0	0.1	0	0	0	0.1	0	0.1	0	0	0.2	0	0	0.1
Ramp Metering	off	off	on	off	off	off	on	off	off	off	off	on	off	off
Speed Control	off	off	off	on	on	on	on	on	on	on	on	off	off	off

Table 1. Ramp flow rates and placement of controllers

Parameters	T_0	N_c	T_1	K_r	K_v	ρ_d	R_{min}	R_{max}	V_{min}	V_{max}	c_v
Values	15s	4	60s	6.48	25	$0.9\rho_c$	480 veh/h	1800 veh/h	45 km/h	105 km/h	30 km/h

Table 2. Controller parameters

We consider five congestion scenarios in our simulations, which could be grouped into two categories: congestion caused by a recurrent bottleneck due to heavy inflows on section 1 of the freeway stretch (we call it peak hour traffic) and congestion caused by a sudden speed drop (we call it accident traffic). Table 3 shows the inputs used in the simulation model to generate these five congestion scenarios.

Scenario #	Scenario Category	Inflow q_d (veh/h/lane)	Disturbance/Incident
1	Peak Hour Traffic (high mainline demand)	2100	None
2	Peak Hour Traffic (high mainline demand)	2200	None
3	Peak Hour Traffic (very high mainline demand)	2300	None
4	Accident Traffic	1800	Speed drops to 10km/h during the time interval 600-900s on section 10 and 11
5	Accident Traffic	1800	Speed drops to 4km/h during the time interval 600-900s on section 10 and 11

Table 3. Simulation inputs for different congestion scenarios

5.2 Evaluation of the IRAC System

Velocity contour plots are chosen to illustrate the simulation results with and without the IRAC system for comparison purposes. For example, in Figure 17, the X axis is time in seconds; the Y axis is distance in station number and the darker the color at point (x, y) is the slower the speed at that point is. From these velocity contour plots, one could easily observe the propagation of shock waves and the changes of speed. In order to quantify the effectiveness of the proposed IRAC system, we use two quantities: Total Time Spent (TTS) in the network and the Standard Deviation of Density (StdK). Environmental effects and safety effects are related to the standard deviation of density since the smoother the density of the segment is, the fewer acceleration or deceleration events take place. Therefore, smaller density deviation is an indicator of lower emission rates and lower possibility of accidents. The TTS (Total Time Spent) is defined as

$$TTS = T_0 \sum_{n=1}^{N_{sim}} \left\{ \sum_{i=4}^N [m_i L_i \rho_i (nT_0)] \right\} \quad (5-3)$$

where $N_{sim}=(3600/T_0)=240$, $N=14$ is the total number of sections. We consider section 4 to 14 for calculating TTS because the first 3 sections of the segment are not controlled via variable speed limits. Moreover, since the inflow to section 1 is at a constant level, if the speed limits are reduced at section 4, the simulation model needs some space to accommodate the extra vehicles which can not enter section 4 and on. Since all the

simulation runs are one hour long and the length of each section is constant, the TTS is actually a weighted measure of the average density of the segment (section 4-14). The standard deviation of density (StdK) which is defined below is a smoothness measure of traffic.

$$\begin{aligned} \text{StdK} &= \text{std}(\rho_{i,n}), \\ \rho_{i,n} &: \text{density of section } i \text{ at time } nT_0 \\ 4 &\leq i \leq 14 \\ 1 &\leq n \leq 240 \end{aligned} \tag{5-4}$$

where $(\rho_{i,n})$ is the density map of the segment (section 4-14) for the whole one hour.

In this section, we present the simulation results obtained when 100% of the vehicles are manually driven. The simulation results of mixed manual and ACC vehicles and 100% ACC vehicles are presented in section 6. When all the vehicles are manually driven, the speed limit commands are communicated to the drivers via billboards or in case of roadway to vehicle communication system via a display or audio inside the vehicle. We assume that drivers will follow the speed limit commands. This is not a strong assumption as only a single driver in each lane needs to respond favorably to the speed limit command to affect the rest.

For the peak hour traffic scenario (scenario 1), section 11 begins to become congested due to the high inflow rate which is approximately close to the estimated capacity. This 4-lane section which has a freeway split becomes a bottleneck due to the immediate on-ramp in the next section. Figure 17(a) indicates how the congestion propagates upstream in the absence of the IRAC system. It cannot be naturally dissipated before reaching the first section of the freeway stretch. The simulation results obtained when the IRAC system is applied are presented in Figure 17(b). When the onset of congestion is detected at section 11, the roadway controller immediately reduces the speed limits of the upstream sections in order to prevent queuing of vehicles at section 11. Therefore, traffic is free flowing shortly after at section 11 and downstream. TTS is reduced to 449veh-h, which means a 13% decrease from the case without the IRAC system (517veh·h). The smoothness of traffic as indicated by the density deviations is also reduced, by a factor of 27% (Table 5). This reduction was acquired by the quick response to the onset of congestion and the smoothness effect of reducing speed limits. Figure 17(b) also shows that congestion seems to be moved from section 11 to section 1-4. This effect is due to the fact that in the simulation, there are no more upstream roadway sections on which traffic could be spread out.

For the accident scenario (scenario 4), a disturbance is generated in sections 10 and 11. At a mild inflow rate, the speed is set to drop to 10km/h between the times of 600s to 900s due to a traffic disturbance. Stop-and-go traffic is generated from the shock waves. The impact of the IRAC system is shown in Figure 18(b). It shows that the speed control strategy yields a homogenization effect on the speed contour. In other words, individual vehicles are not forced to decelerate dramatically. TTS is reduced to 624veh-h, which

means a 10% decrease due to the use of the IRAC system than without it (692veh·h). Density deviations are reduced by 11% (Table 5) due to the IRAC system. Since the controller makes the stop-and-go traffic smoother, it reduces the chance of rear-end collisions caused by sudden decelerations. The emissions are also expected to be reduced since the acceleration and deceleration events occur less frequently.

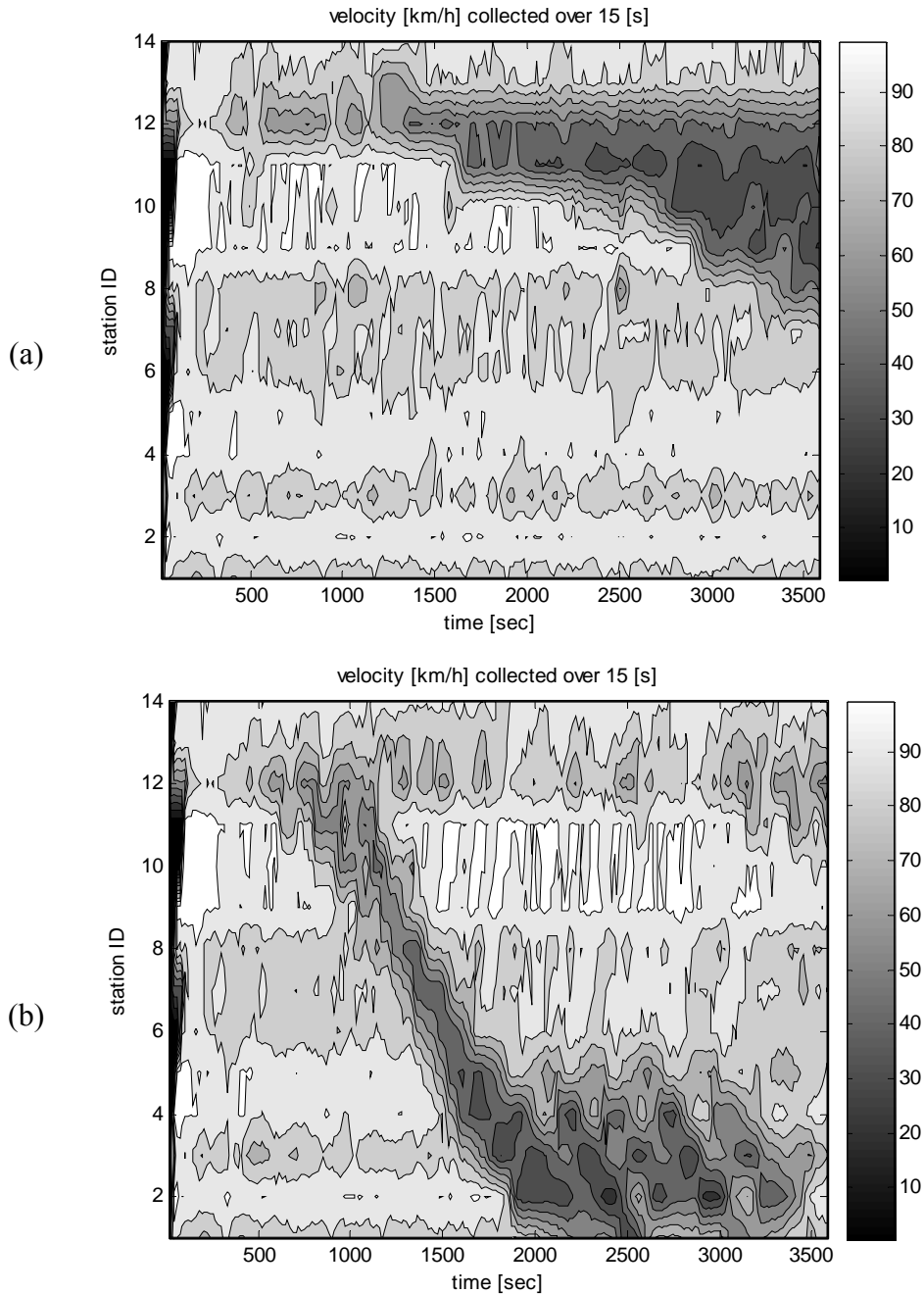


Figure 17: Speed contours for scenario 1: (a) Without IRAC and (b) With IRAC

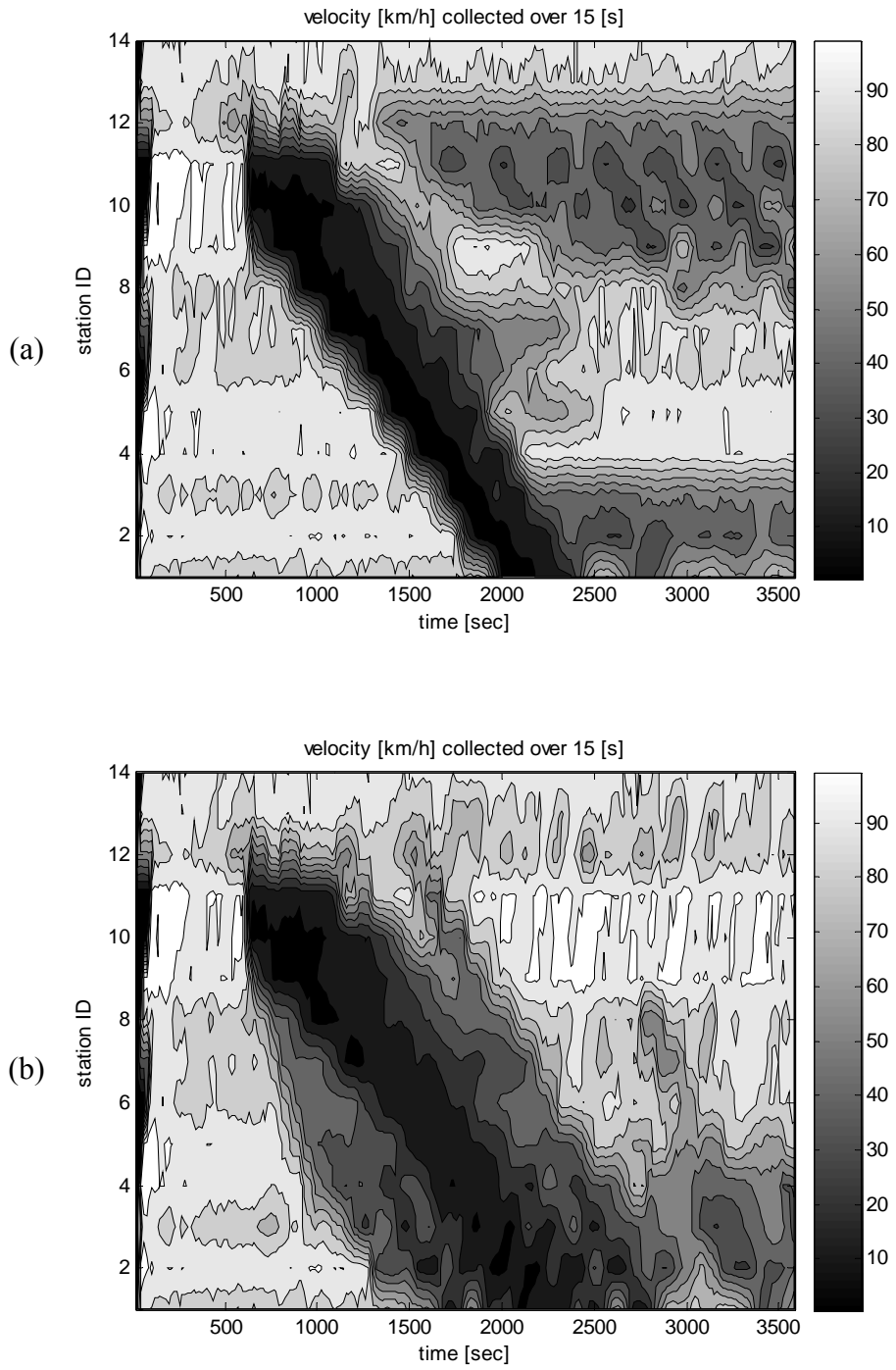


Figure 18: Speed contours for scenario 4: (a) Without IRAC and (b) With IRAC

6 UPGRADING THE IRAC SYSTEMS

In this section we assume that vehicles with Adaptive Cruise Control (ACC) capabilities are present operating together with manually driven vehicles. The roadway communicates directly with the ACC controller which responds to the speed limit commands without having to rely on the driver. The presence of ACC vehicles has several benefits. First the ACC vehicles help smooth the traffic flow by filtering traffic disturbances. Second they could employ smaller headways which will help increase capacity and third by obeying the speed limit commands they help with compliance as the ACC vehicle dictates the speed of the lane for all following vehicles.

6.1 Effect of ACC Vehicles on Flow-Density Relationship

After validating the VISSIM freeway model using BHL field data, we also estimated critical densities and capacity flows and other traffic flow characteristics for mixed manual and ACC vehicles scenarios. Figure 19 shows that the critical density and capacity increase with the ACC penetration while the shape of the fundamental diagram remains the same during the free flow region which agrees with intuition.

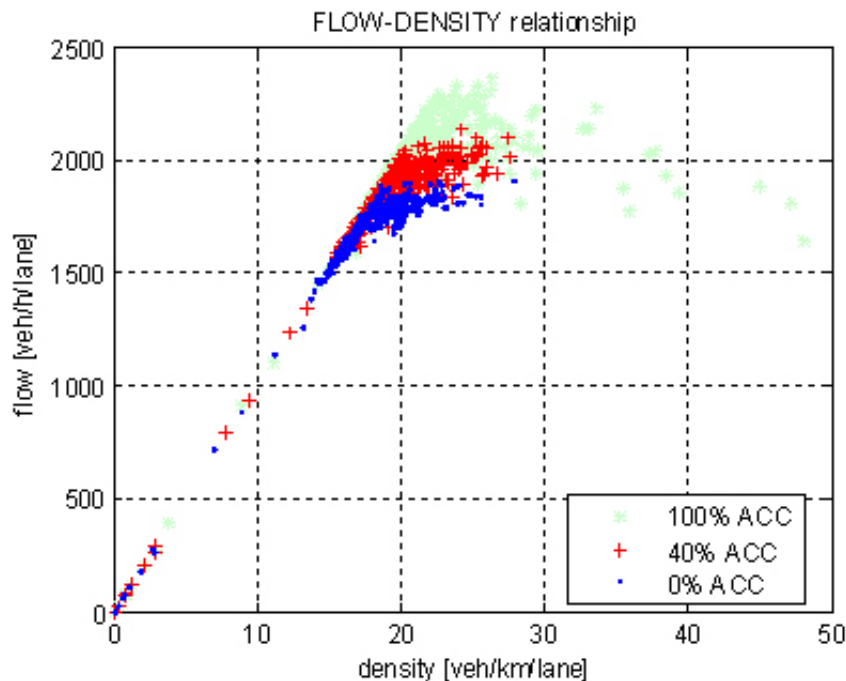
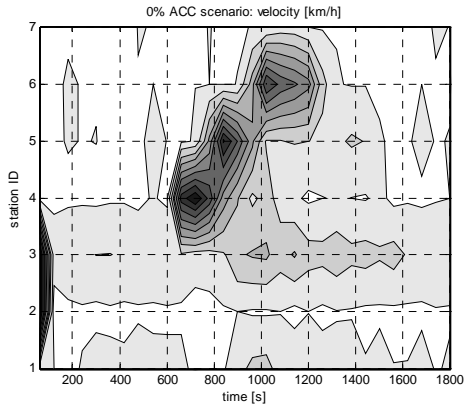


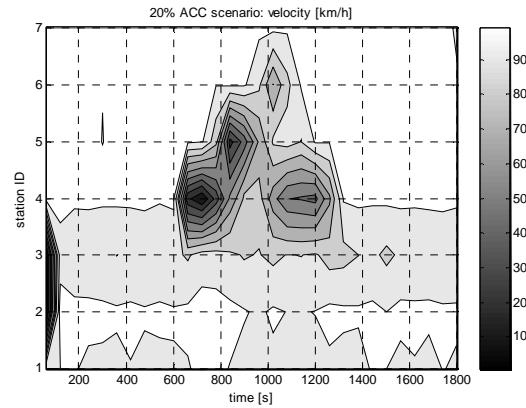
Figure 19: Flow-density diagram in mixed ACC scenarios

We already observed that shock waves travel faster in mixed traffic than in manual traffic [43]. To investigate this effect using our microscopic model, the speed of shock waves is evaluated by generating disturbances in a downstream section. Figure 20 shows the speed

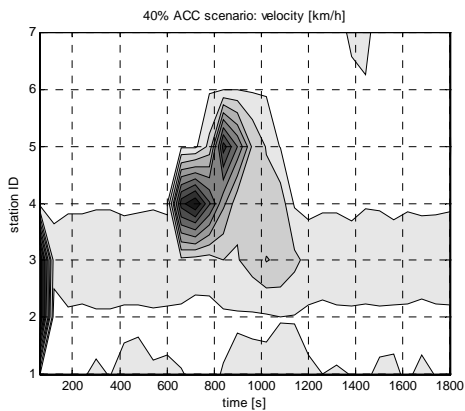
contour of simulation runs with different ACC penetration levels. These speed contour plots illustrate the propagation pattern of the shock waves. It is observed that the duration of shock waves decreases as the penetration of the ACC vehicles increases. It is also observed that the speeds of the shock waves increase as the penetration of ACC vehicles increases. Table 4 summarizes shock wave speeds estimated from vehicle trajectories for different mixed vehicle scenarios.



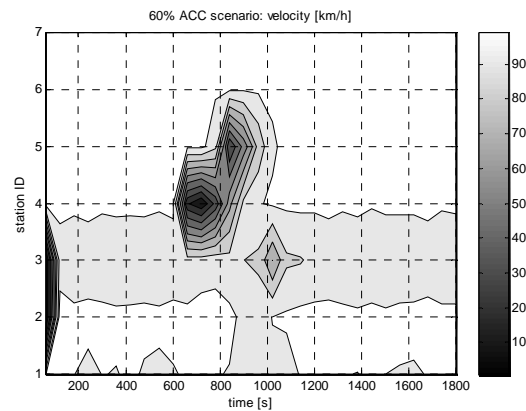
(a)



(b)



(c)



(d)

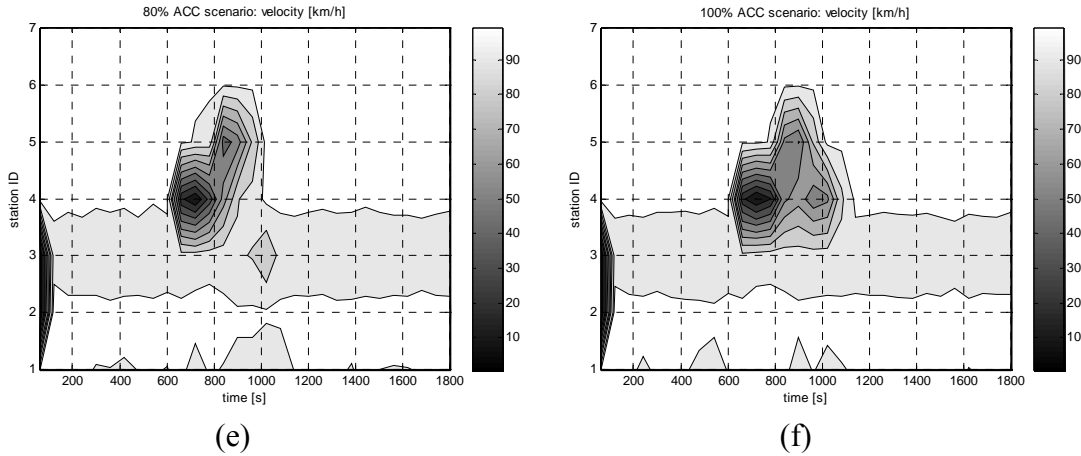


Figure 20: Propagation of shock waves (a) 0% ACC vehicles (b) 20% ACC (c) 40% ACC (d) 60% ACC (e) 80% ACC (f) 100% ACC

Penetration of ACC vehicles [%]	Speed of shock wave [m/s]
0	2.67
20	2.80
40	2.85
60	3.12
80	3.33
100	3.75

Table 4. Shock wave speeds of different traffic composition

It is clear from the results of the table that the shock wave travels faster and therefore reaches the points of diffusion faster in the case of ACC vehicles. The reason is that the ACC vehicles react faster to speed changes than individual drivers.

Let us now compare the trajectories of some vehicles in manual and mixed traffic simulation runs in Figure 21. All vehicles start at approximately the same location and time. It is found that the presence of semi-automated vehicles does not affect the total travel time during traffic disturbances.

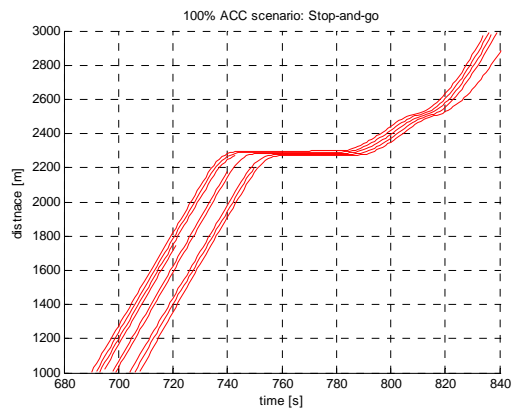
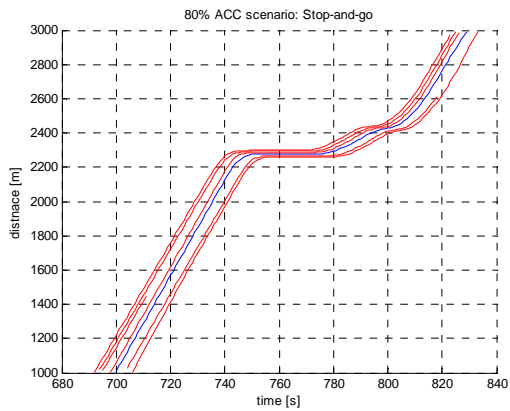
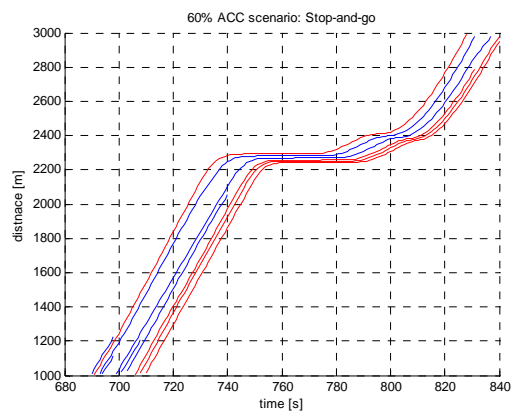
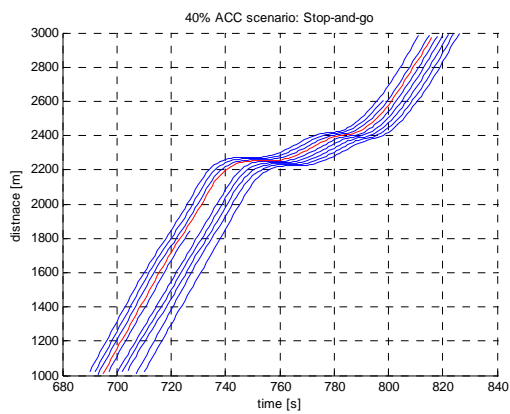
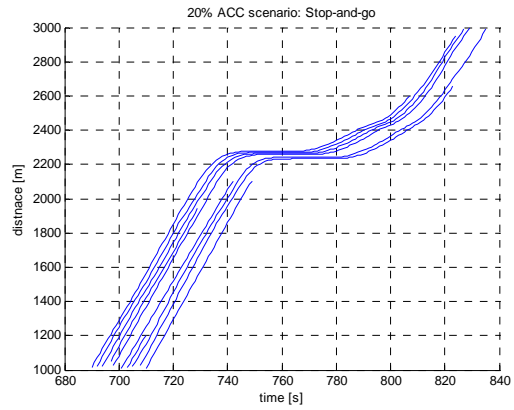
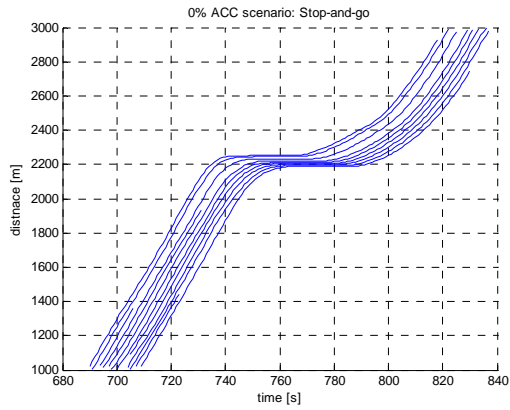


Figure 21: Selected vehicle trajectories (a) 0% ACC vehicles (b) 20% ACC (c) 40% ACC (d) 60% ACC (e) 80% ACC (f) 100% ACC. Red lines represent ACC vehicles and Blue lines represent manual vehicles.

6.2 Controller Simulation Results with ACC Vehicles

In this section we examine the properties of the IRAC system for different ACC penetration levels using the same congestion scenarios as in section 5.2. Figure 22 (c) and (d) are speed contour plots of simulations runs for congestion scenario 1 when 40% of the vehicles are ACC vehicles without and with the IRAC system, respectively. Figure 22 (e) and (f) are speed contour plots of simulations runs for congestion scenario 1 when all the vehicles are ACC vehicles with and without the IRAC system, respectively. Figure 22(a) and (b) are the same plots from section 5.2, included here for the purpose of comparison. Table 5 summarizes the TTS and StdK values for all the simulations runs. (These values are the average values of simulation runs with at least four different random seeds.) Keeping in mind that as the percentage of ACC vehicles increases the capacity and the critical density of the roadway increases, it is not surprising to find out that with 100% ACC vehicles, the congestion is almost gone even without the use of the roadway controller. Therefore, the controller did not improve TTS very much when all the vehicles are ACC vehicles. Since our controllers depend on the critical density, for different ACC rates, we used different critical density in our simulations which are also summarized in table 5.

Figure 23 shows the propagation of shock waves which are caused by the disturbance (scenario 4). TTS and StdK are both decreased as a result of the IRAC system. This homogenization effect has beneficial effects on the environment, fuel economy and stability of traffic flow as also pointed out in previous studies [44].

ACC%		0% ($\rho_c=27$)		10% ($\rho_c=29$)		40% ($\rho_c=31$)		100% ($\rho_c=36$)	
		TTS (veh·h)	StdK (veh/km)	TTS (veh·h)	StdK (veh/km)	TTS (veh·h)	StdK (veh/km)	TTS (veh·h)	StdK (veh/km)
Scenario #									
1	w/o IRAC	517	9.44	489.5	8.44	491.6	7.94	463.3	5.53
	with IRAC	448.5	6.86	460	6.85	476.2	6.86	456.2	5.1
	down by	13%	27%	6%	19%	3%	14%	2%	8%
2	w/o IRAC	555.1	10.23	541.3	9.92	498.8	8.31	549.6	8.81
	with IRAC	455.7	7.41	470.1	7.2	471.6	6.78	527.2	8.05
	down by	18%	28%	13%	27%	5%	18%	4%	9%
3	w/o IRAC	548.8	10.17	533.3	9.78	501.4	8.08	537.2	8.08
	with IRAC	454.6	7.14	468.5	7.24	481.7	7.01	496.4	6.78
	down by	17%	30%	12%	26%	4%	13%	8%	16%
4	w/o IRAC	692.4	21.94	694.8	21.08	670.7	20.21	654.8	21.52
	with IRAC	624.3	19.46	622.6	19.27	621.8	19.76	642.8	19.97
	down by	10%	11%	10%	9%	7%	2%	2%	7%
5	w/o IRAC	969.8	35.98	1017.7	36.75	938.9	35.31	1091.8	41.12
	with IRAC	793.7	33.21	881.5	34.48	871.3	34.51	944.4	36.31
	down by	18%	8%	13%	6%	7%	2%	14%	12%

Table 5. All simulation results

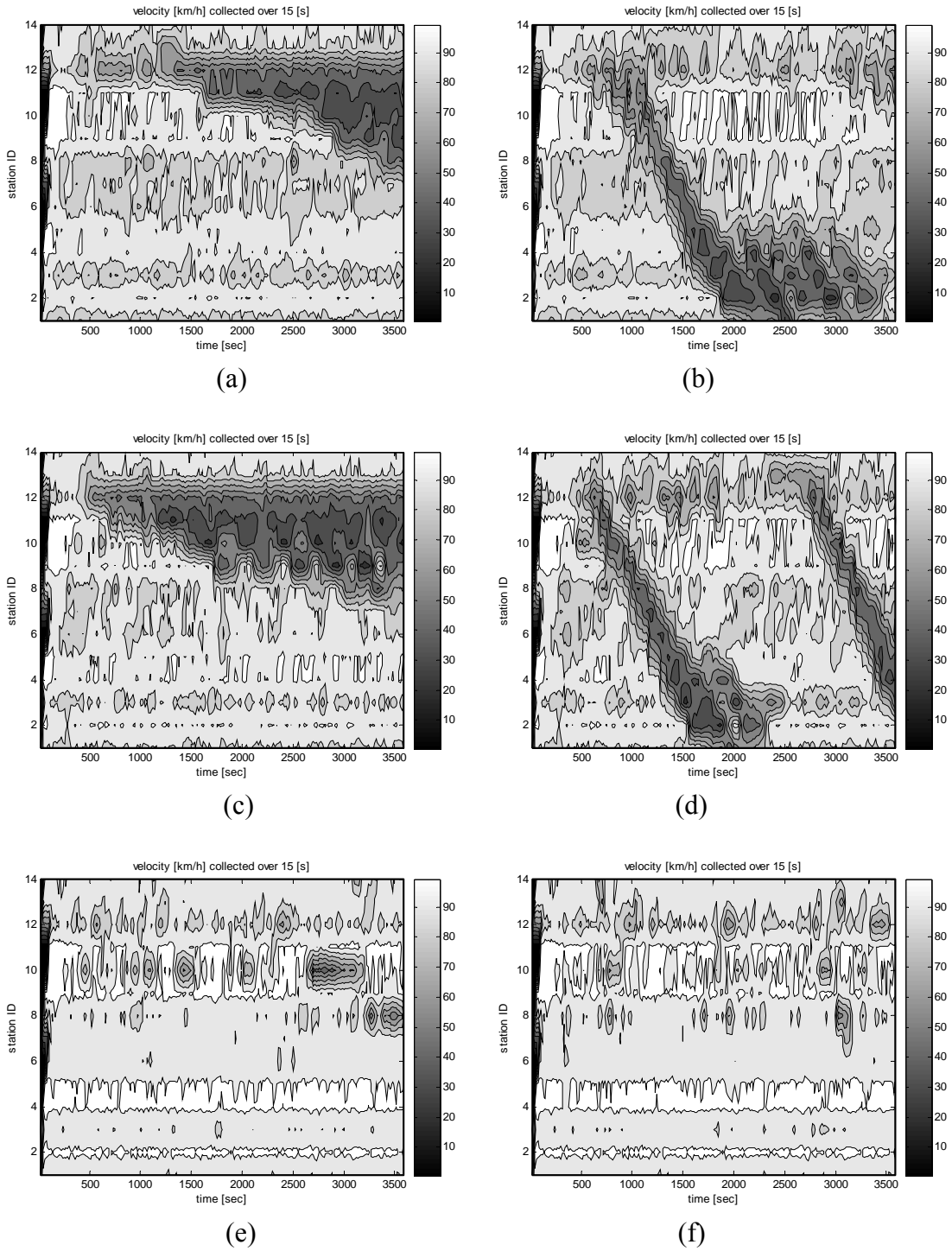
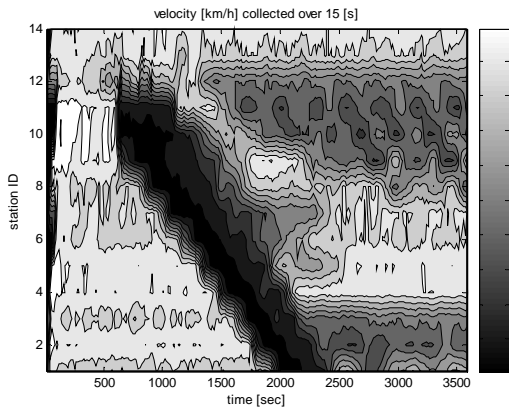
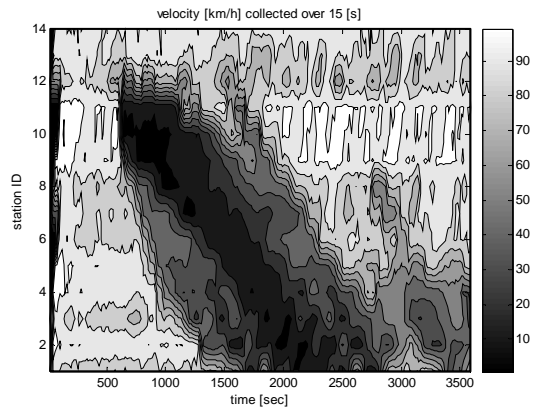


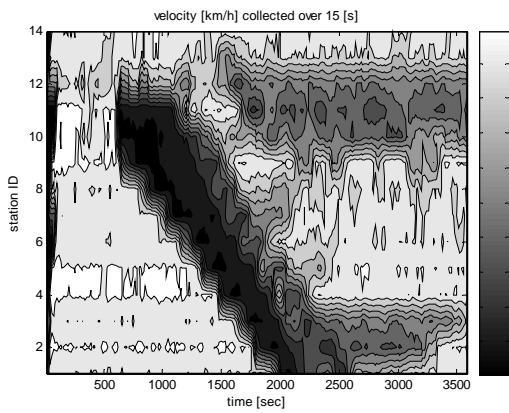
Figure 22: Speed contour of scenario 1 (a) 0% ACC, w/o IRAC (b) 0% ACC, with IRAC (c) 40% ACC, w/o IRAC (d) 40% ACC, with IRAC (e) 100% ACC, w/o IRAC (f) 100% ACC, with IRAC



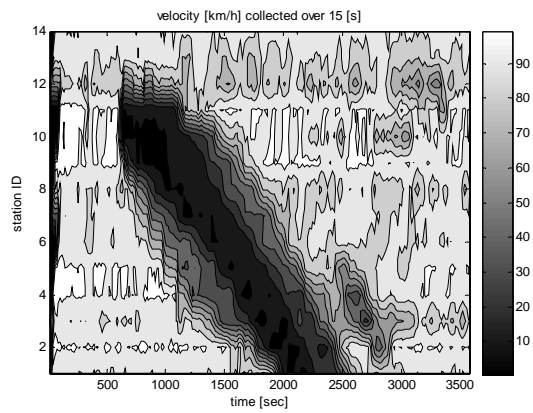
(a)



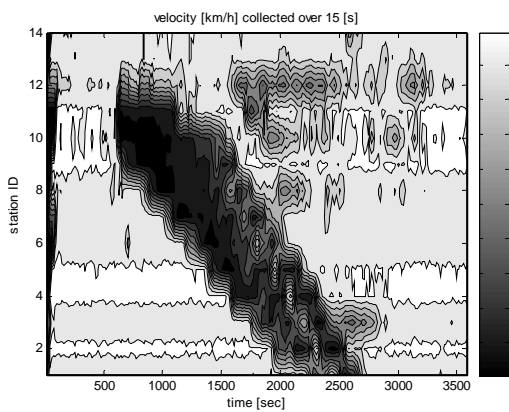
(b)



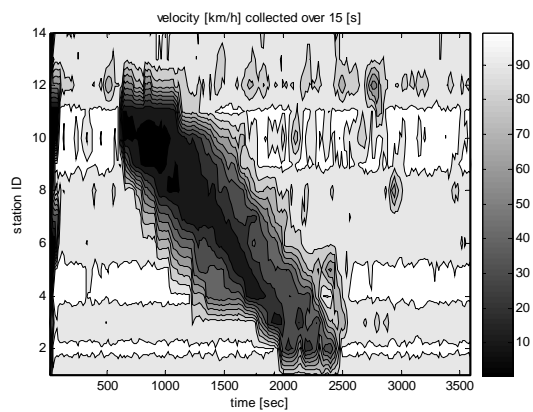
(c)



(d)



(e)



(f)

Figure 23: Speed contour of scenario 4 (a) 0% ACC, w/o IRAC (b) 0% ACC,with IRAC (c) 40% ACC, w/o IRAC (d) 40% ACC, with IRAC (e) 100% ACC, w/o IRAC (f) 100% ACC, with IRAC

7 DEPLOYMENT OF THE IRAC SYSTEM

The IRAC system is demonstrated using a validated simulation model to improve traffic flow characteristics and efficiency with positive impact on travel time, safety and environment. The next step is to demonstrate these benefits by deploying it and evaluating its performance. A segment of I-80, just north of Bay Bridge, California is proposed as a possible deployment site. The reason is that section 2 through 7 of that segment is part of the BHL and therefore traffic data are readily available for model validation and studies. In addition, billboards or communication beacons can be easily installed at the beginning of each section from section 3 to section 12, at the locations of detector stations and billboards or beacons shown in Figure 24.

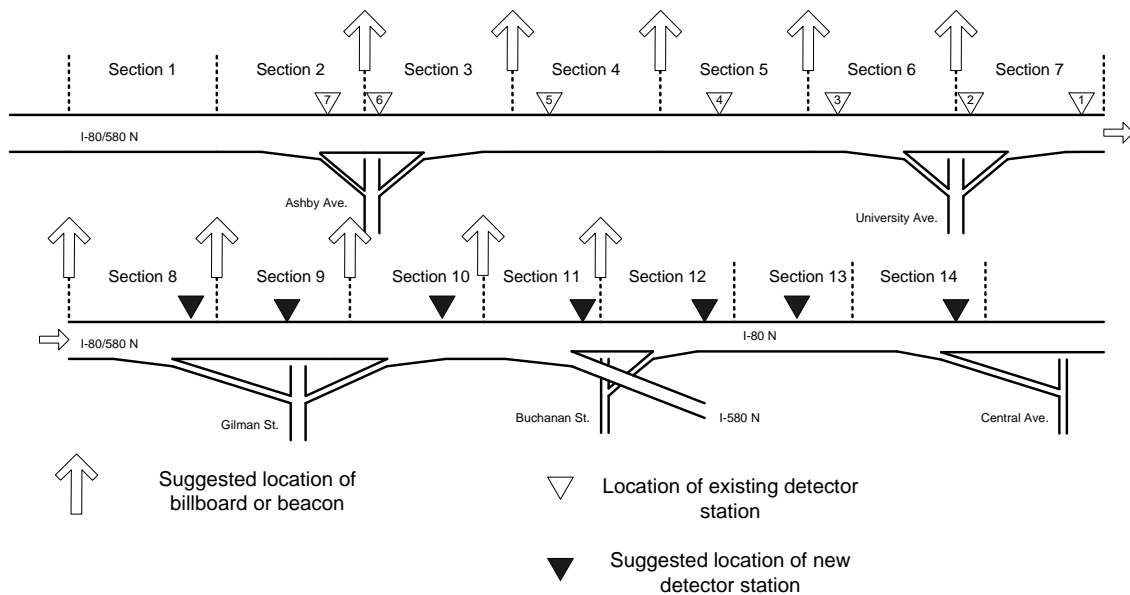


Figure 24: Suggested locations of detector stations and locations of billboards or beacons along the I-80 segment.

While many other deployment sites are possible the proposed site requires much less changes due to the availability of sensors and data collection capabilities as part of BHL.

8 CONCLUSIONS

In this project, link layer controllers are developed to interface with the ACC vehicles and manual vehicles. The purpose of the roadway or link layer controller is to control traffic flow by sending appropriate commands to individual vehicles at the various sections along the highway in addition to ramp metering. The roadway commands include desired speeds to be followed by vehicles at different sections communicated directly to the ACC vehicles for the purpose of harmonizing traffic flow and improving its rate and for safety due to downstream environmental and traffic conditions.

We use a simple and efficient roadway control system which is composed of a ramp metering strategy and a speed control strategy. The ramp metering strategy is a generalized version of ALINEA. The speed control strategy treats the speed limit for one freeway section as a virtual ramp meter for the next downstream freeway section, and it is designed only based on the fundamental flow-density relationship

The idea of communicating desired speed to manual vehicles includes variable message signs along the freeway. Also, in order to implement the direct communication to ACC vehicles, we define the adopted dedicated short range communication (DSRC) system.

The integrated Roadway/ACC system is evaluated on a freeway model using a microscopic traffic simulation tool VISSIM which is popularly used to model a surface transportation network at a high level of details. The model was based on a stretch of the highway Interstate 80 and its driving behavior parameters were calibrated using measured field data from the Berkeley Highway Laboratory (BHL). After the BHL model was validated, it was extended to include several more ramps from its downstream. Also, we estimated critical densities, capacity flows and other traffic flow characteristics for mixed manual and ACC vehicles scenarios. Simulation results of different congestion scenarios demonstrate that the designed controller can efficiently dissipate congestions, improve safety and significantly reduce the total time spent (TTS) in the network. In case of an accident in downstream which causes a sudden block of the freeway section, simulation result shows that the controller yields more stable traffic by reducing the speed differences in upstream. In case of high traffic demands, we observed that the controller could effectively relieve congestion and improve TTS.

REFERENCES

- [1] Papageorgiou M. and Kotsialos A., "Freeway ramp metering: an overview," *IEEE Transactions on Intelligent Transportation Systems*, vol. 3, no. 4, pp 271-281, 2002.
- [2] Papageorgiou M., Hadj-Salem H., and Blosseville J.-M., "ALINEA: a local feedback control law for on-ramp metering," *Transportation Research Record*, 1991, No. 1320, pp. 58-64.
- [3] Smaragdis E., Papageorgiou M., and Kosmatopoulos E., "A flow-maximizing adaptive local ramp metering strategy", *Transportation Research Part B*, vol. 38, pp. 251-270, 2004.
- [4] Papageorgiou M., Haj-Salem H., and Middleham F., "ALINEA local ramp metering: summary of field results", *Transportation Research Record*, No. 1603, pp. 90-98, 1997.
- [5] Hegyi A., Schutter B. D., and Hellendoorn H., "Model predictive control for optimal coordination of ramp metering and variable speed limits", *Transportation Research Part C*, vol. 13, pp 185-209, 2005.
- [6] Kotsialos A., Papageorgiou M., Mangeas M., and Haj-Salem H., "Coordinated and integrated control of motorway networks via nonlinear optimal control," *Transportation Research Part C*, vol. 10, pp. 65-84, 2002.
- [7] Chang T. and Li Z., "Optimization of mainline traffic via an adaptive coordinated ramp-metering control model with dynamic OD estimation", *Transportation Research Part C*, Vol. 10, pp. 99-120, 2002.
- [8] Zhang H. M., Ritchie S. G. and Jayakrishnan R., "Coordinated traffic-responsive ramp control via nonlinear state feedback", *Transportation Research Part C*, Vol. 9, pp. 337-352, 2001.
- [9] Zhang H. M., Ritchie S.G., and Recker W., "Some general results on the optimal ramp metering control problem," *Transportation Research Part C*, vol. 4, pp 51-69, 1996.
- [10] Stephanedes Y. and Chang K.-K., "Optimal control of freeway corridors," *ASCE J. Transportation Eng.*, vol. 119, pp. 504-514, 1993.
- [11] Papageorgiou M. and Mayr R., "Optimal decomposition methods applied to motorway traffic control," *Int. J. Control*, vol. 35, pp. 269-280, 1982.
- [12] Smulders S. A., "Control of freeway traffic by variable speed signs," *Transportation Research Part B*, vol. 24(2), pp. 111-132, 1990.

- [13] Mammar S., Messmer A., Jensen P., Papageorgiou M., Haj-Salem H., and Jensen L., "Automatic control of variable message signs in Aalborg," *Transportation Research Part C*, vol. 4(3), pp. 131-150, 1996.
- [14] Chien C. C., Zhang Y., and Ioannou P.A., "Traffic density control for automated highway systems," *Automatica*, vol. 33, no. 7, pp. 1273-1285, 1997.
- [15] Alessandri A. , Di Febbraro A., Ferrara A., and Punta E., "Nonlinear optimization for freeway control using variable-speed signaling," *IEEE Transactions on Vehicular Technology*, vol. 48, no. 6, pp. 2042-2052, 1999.
- [16] Hegyi A., De Schutter B., Hellendoorn H., and Van Den Boom T., "Optimal coordination of ramp metering and variable speed control – an MPC approach," *Proceedings of the 2002 American Control Conference*, Anchorage, Alaska, May 2002, pp. 3600-3605.
- [17] Zhang J., Boitor A., and Ioannou P.A., "Design and evaluation of a roadway controller for freeway traffic," *Proceedings of the 8th International IEEE Conference on Intelligent Transportation Systems*, Vienna, Austria, 2005, pp. 543-548.
- [18] Chang H., Wang Y., Zhang J., and Ioannou P.A., "An integrated roadway controller and its evaluation by microscopic simulator VISSIM," *submitted to European Control Conference 2007*, Kos, Greece, July 2007.
- [19] Ioannou P.A., *Automated Highway Systems*, Plenum Press, New York, 1997.
- [20] Jones W.D., "Building safer cars," *IEEE Spectrum*, vol. 39, no. 1, Jan. 2002, pp. 82-85.
- [21] Richard B., "Japan's Demo 2000 Wows Attendees," *ITS World*, January/February 2001, pp. 18-19.
- [22] Zhang J. and Ioannou P., "Integrated Roadway / Adaptive Cruise Control System: Safety, Performance, Environmental and Near Term Deployment Considerations," *California PATH Research Report*, UCB-ITS-PRR-2004-32, Sept. 2004.
- [23] Hasan M., Jha M. and Ben-Akiva M., "Evaluation of ramp control algorithms using microscopic traffic simulation," *Transportation Research Part C*, vol. 10, pp. 229-256, 2002.
- [24] Wang Y. and Ioannou P., "Real-time parallel parameter estimators for a second-order macroscopic traffic flow model", in *Proceedings of the 9th IEEE Intelligent Transportation Systems Conference*, Toronto, Canada, 2006, pp. 1466-1470.

- [25] National ITS Architecture webpage:
<http://itsarch.iteris.com/itsarch/html/entity/paents.htm>
- [26] Liu Y., Dion F. and Biswas S., “Dedicated Short-Range Wireless Communications for Intelligent Transportation System Applications: State of the Art”, *Transportation Research Record: Journal of the Transportation Research Board*, No. 1910, pp 29-37.
- [27] Crash Avoidance Metrics Partnership; National Highway Traffic Safety Administration, “Vehicle Safety Communications Project Task 3 Final Report—Identify Intelligent Vehicle Safety Applications Enabled by DSRC”, March 2005.
- [28] Traffic analysis toolbox, Federal Highway Administration, U.S. Department of Transportation, June 2004.
- [29] The Berkeley Highway Laboratory webpage:
<http://bhl.its.berkeley.edu:9006/bhl/index.html>
- [30] TSIS-CORSIM, Federal Highway Administration.
<http://mctrans.ce.ufl.edu/featured/TSIS/>
- [31] VISSIM, PTV AG.
http://www.english.ptv.de/cgi-bin/traffic/traf_vissim.pl
- [32] Bloomberg L. and Dale J., “A comparison of VISSIM and CORSIM traffic simulation models,” *Institute of Transportation Engineers Annual Meeting*, August 2000.
- [33] Bloomberg L. and Dale J., “A comparison of VISSIM and CORSIM traffic simulation models on a congested network, *Transportation Research Record*, no. 1727, pp. 52-60, 2000.
- [34] Tian Z., Urbanik T., Engelbrecht R., and Balke K., “Variations in capacity and delay estimates from microscopic traffic simulation models, *Transportation Research Record*, no. 1802, pp. 23-31, 2002.
- [35] Gomes G., May A., and Horowitz R., “A micro simulation model of a congested freeway using VISSIM,” *Transportation Research Board Conference*, Nov. 2004.
- [36] Trueblood M. and Dale J., “Simulating roundabouts with VISSIM,” *the 2nd Urban Street Symposium*, Anaheim, California, July 2003.
- [37] Fellendorf M. and Vortisch P., “Validation of the Microscopic Traffic Flow Model VISSIM in Different Real-World Situations,” *the 80th TRB Annual Meeting*, Washington, DC, 2001.

- [38] Wiedemann R., Simulations des Straßenverkehrsflusses, Schriftenreihe des Instituts für Verkehrswesen der Universität Karlsruhe, Heft 8, 1974.
- [39] Wiedemann R., "Modeling of RTI-Elements on multi-lane roads," In: *Advanced Tematics in Road Transport edited by the Comission of the European Community*, XIII, Brussels, 1991.
- [40] Highway Capacity Manual 2000, Transportation Research Board, December 2000.
- [41] The MathWorks, Inc., External Interface.
http://www.mathworks.com/access/helpdesk/help/techdoc/matlab_external/
- [42] User manual for the VISSIM COM interface, PTV AG, 2006.
- [43] Bose A., Ioannou P., "Mixed Manual/Semi-Automated Traffic: A Macroscopic Analysis", *California PATH Research Report*, UCB-ITS-PRR-2001-14, 2001.
- [44] Hegyi A., De Schutter B. and Hellendoorn H., "Optimal coordination of variable speed limits to suppress shock waves", *Transportation Research Record* (1852), pp.167-174.
- [45] PATH Research <http://www.path.berkeley.edu/>
- [46] Ioannou, P. Automated Highway Systems. Plenum, 1997.
- [47] Shladover S., "Review of the State of Development of Advanced Vehicle Control Systems (AVCS)", *Vehicle System Dynamics*, Swets & Zeitlinger, 24, pp. 551-595, 1995.
- [48] Bishop, J. and W. Stevens 'Results of precursor systems analyses of automated highway systems' *Proc. First World Congress on Applications of Transport Telematics and Intelligent Vehicle*, 1997.
- [49] Zhang W.B., "National Automated Highway System Demonstration: A Platoon System", *the IEEE Conference on Intelligent Transportation Systems*, Boston, Massachusetts, Nov. 1997.
- [50] Thorpe C., Jochem T. and D. Pomerleau, "The 1997 Automated Highway Free Agent Demonstration", *the IEEE Conference on Intelligent Transportation Systems*, Boston, Massachusetts, Nov. 1997.
- [51] Fancher P. et.al. "Data Processing Procedures for Identifying driver/Vehicle Properties Associated with the Control of Headway", the 1997 Automated Highway Free Agent Demonstration, *the IEEE Conference on Intelligent Transportation Systems*, Boston, Massachusetts, Nov. 1997.

- [52] Hedrick J., M. Tomizuka and P. Varaiya, "Control issues in automated highway systems", *IEEE Controls System Magazine*, Dec. 1994.
- [53] Varaiya P. "Smart cars on smart roads: Problems of control", *IEEE Trans. Automatic Control*, Vol. 38, pp. 195-207, 1993
- [54] Ioannou P., "Evaluation and Analysis of Automated Highway Concepts and Architecture", *California PATH Reports to Caltrans 99-C6*, Aug. 1999.
- [55] C. Chen, Z. Jia and P. Varayia, "Causes and cures of highway congestion", *IEEE Controls Systems Magazine*, 21(4), pp26-33, Dec. 2001